

---

# Neutron Scattering Studies of Antiferromagnetic Correlations in Cuprates

John M. Tranquada

Physics Department, Brookhaven National Laboratory, Upton, NY 11973, USA

**Summary.** Neutron scattering studies have provided important information about the momentum and energy dependence of magnetic excitations in cuprate superconductors. Of particular interest are the recent indications of a universal magnetic excitation spectrum in hole-doped cuprates. That starting point provides motivation for reviewing the antiferromagnetic state of the parent insulators, and the destruction of the ordered state by hole doping. The nature of spin correlations in stripe-ordered phases is discussed, followed by a description of the doping and temperature dependence of magnetic correlations in superconducting cuprates. After describing the impact on the magnetic correlations of perturbations such as an applied magnetic field or impurity substitution, a brief summary of work on electron-doped cuprates is given. The chapter concludes with a summary of experimental trends and a discussion of theoretical perspectives.

## 8.1 Introduction

Neutron scattering has played a major role in characterizing the nature and strength of antiferromagnetic interactions and correlations in the cuprates. Following Anderson's observation [1] that  $\text{La}_2\text{CuO}_4$ , the parent compound of the first high-temperature superconductor, should be a correlated insulator, with moments of neighboring  $\text{Cu}^{2+}$  ions anti-aligned due to the superexchange interaction, antiferromagnetic order was discovered in a neutron diffraction study of a polycrystalline sample [2]. When single-crystal samples became available, inelastic studies of the spin waves determined the strength of the superexchange,  $J$ , as well as weaker interactions, such as the coupling between  $\text{CuO}_2$  layers. The existence of strong antiferromagnetic spin correlations above the Néel temperature,  $T_N$ , has been demonstrated and explained. Over time, the quality of such characterizations has improved considerably with gradual evolution in the size and quality of samples and in experimental techniques.

Of course, what we are really interested in understanding are the optimally-doped cuprate superconductors. It took much longer to get a clear picture of the magnetic excitations in these compounds, which should not be surprising

given that there is no static magnetic order, the magnetic moments are small, and the bandwidth characterizing the magnetic excitations is quite large. Nevertheless, we are finally at a point where a picture of universal behavior, for at least two families of cuprates, is beginning to emerge. Thus, it seems reasonable to start our story with recent results on the excitation spectrum in superconducting  $\text{YBa}_2\text{Cu}_3\text{O}_{6+x}$  and  $\text{La}_{2-x}\text{Sr}_x\text{CuO}_4$ , and the nature of the spin gap that appears below the superconducting transition temperature,  $T_c$ . (Note that these are hole-doped superconductors, which is where most of the emphasis will be placed in this chapter.) An important result is that this spectrum looks quite similar to that measured for  $\text{La}_{1.875}\text{Ba}_{0.125}\text{CuO}_4$ , a compound in which  $T_c$  is depressed towards zero and ordered charge and spin stripes are observed. The nature of stripe order and its relevance will be discussed later.

Following the initial discussion of results for the superconductors in §8.2, one can have a better appreciation for the antiferromagnetism of the parent insulators, presented in §8.3. The destruction of antiferromagnetic order by hole doping is discussed in §8.4. In §8.5, evidence for stripe order, and for other possible ordered states competing with superconductivity, is considered. §8.6 discusses how the magnetic correlations in superconducting cuprates evolve with hole-doping and with temperature. While doping tends to destroy antiferromagnetic order, perturbations of the doped state can induce static order, or modify the dynamics, and these effects are discussed in §8.7. A brief description of work on electron-doped cuprates is given in §8.8. The chapter concludes with a discussion, in §8.9, of experimental trends and theoretical perspectives on the magnetic correlations in the cuprates. It should be noted that there is not space here for a complete review of neutron studies of cuprates; some earlier reviews and different perspectives appear in Refs. [3, 4, 5, 6, 7, 8].

Before getting started, it is useful to first establish some notation. A general wave vector  $\mathbf{Q} = (h, k, l)$  is specified in units of the reciprocal lattice,  $(a^*, b^*, c^*) = (2\pi/a, 2\pi/b, 2\pi/c)$ . The  $\text{CuO}_2$  planes are approximately square, with a Cu-Cu distance of  $a \approx b \sim 3.8 \text{ \AA}$ . Antiferromagnetic order of Cu moments ( $S = \frac{1}{2}$ ) in a single plane causes a doubling of the unit cell and is characterized by the wave vector  $\mathbf{Q}_{\text{AF}} = (\frac{1}{2}, \frac{1}{2}, 0)$ , as indicated in Fig. 8.1; however, the relative ordering of the spins along the  $c$  axis can cause the intensities of  $(\frac{1}{2}, \frac{1}{2}, L)$  superlattice peaks to have a strongly modulated structure factor as a function of  $L$ . For the magnetic excitations, we will generally be interested in their dependence on  $\mathbf{Q}_{2\text{D}} = \mathbf{Q} - (\frac{1}{2}, \frac{1}{2}, L)$  associated with an individual  $\text{CuO}_2$  plane and ignoring the  $L$  dependence.

The magnetic scattering function measured with neutrons can be written as [9, 10]

$$\mathcal{S}(\mathbf{Q}, \omega) = \sum_{\alpha, \beta} (\delta_{\alpha, \beta} - Q_\alpha Q_\beta / Q^2) S^{\alpha\beta}(\mathbf{Q}, \omega), \quad (8.1)$$

where

$$S^{\alpha\beta}(\mathbf{Q}, \omega) = \frac{1}{2\pi} \int_{-\infty}^{\infty} dt e^{-i\omega t} \sum_{\mathbf{r}} e^{i\mathbf{Q} \cdot \mathbf{r}} \langle S_{\mathbf{0}}^\alpha(0) S_{\mathbf{r}}^\beta(t) \rangle. \quad (8.2)$$

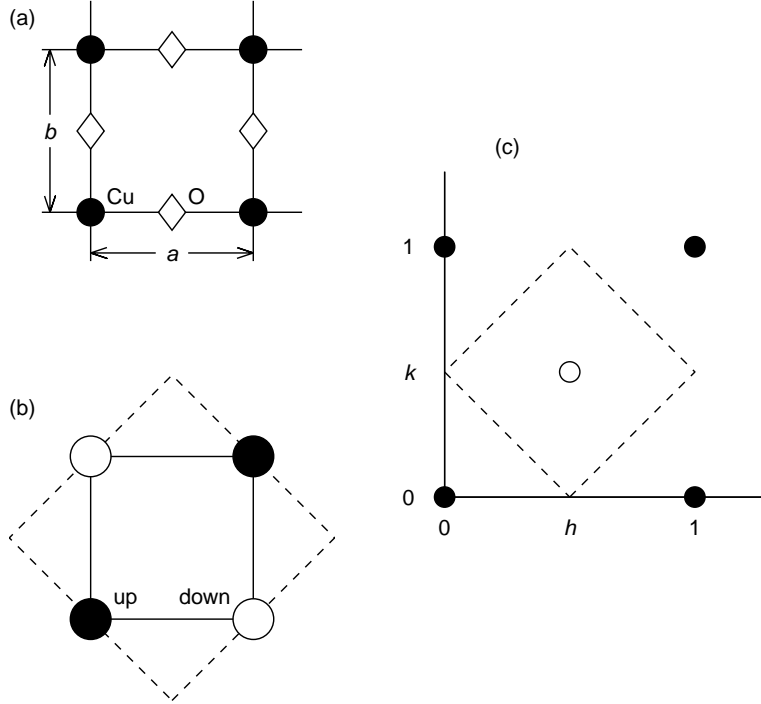


**Fig. 8.1.** (a)  $\text{CuO}_2$  plane, indicating positions of the Cu and O atoms and identifying the lattice parameters,  $a$  and  $b$ . (b) Sketch of antiferromagnetic order of Cu moments, with filled (empty) circles representing up (down) spins. Solid line indicates the chemical unit cell; dashed line denotes the magnetic unit cell. (c) Filled circles: Bragg peak positions in reciprocal space corresponding to the chemical lattice. Empty circle: magnetic Bragg peak due to antiferromagnetic order. Dashed line indicates the antiferromagnetic Brillouin zone.

Here  $S_{\mathbf{r}}^{\beta}(t)$  is the  $\beta$  ( $= x, y, z$ ) component of the atomic spin at lattice site  $\mathbf{r}$  and time  $t$ , and the angle brackets,  $\langle \dots \rangle$  denote an average over configurations. For inelastic scattering, it is possible to relate  $\mathcal{S}(\mathbf{Q}, \omega)$  to the imaginary part of the dynamical spin susceptibility,  $\chi''(\mathbf{Q}, \omega)$  via the fluctuation-dissipation theorem,

$$\mathcal{S}(\mathbf{Q}, \omega) = \frac{\chi''(\mathbf{Q}, \omega)}{1 - e^{-\hbar\omega/k_{\text{B}}T}}. \quad (8.3)$$

Another useful quantity is the “local” susceptibility  $\tilde{\chi}''(\omega)$ , defined as

$$\tilde{\chi}''(\omega) = \int d\mathbf{Q}_{2\text{D}} \chi''(\mathbf{Q}, \omega). \quad (8.4)$$

Experimentally, the integral is generally not performed over the entire first Brillouin zone, but rather over the measured region about  $\mathbf{Q}_{\text{AF}}$ .

## 8.2 Magnetic excitations in hole-doped superconductors

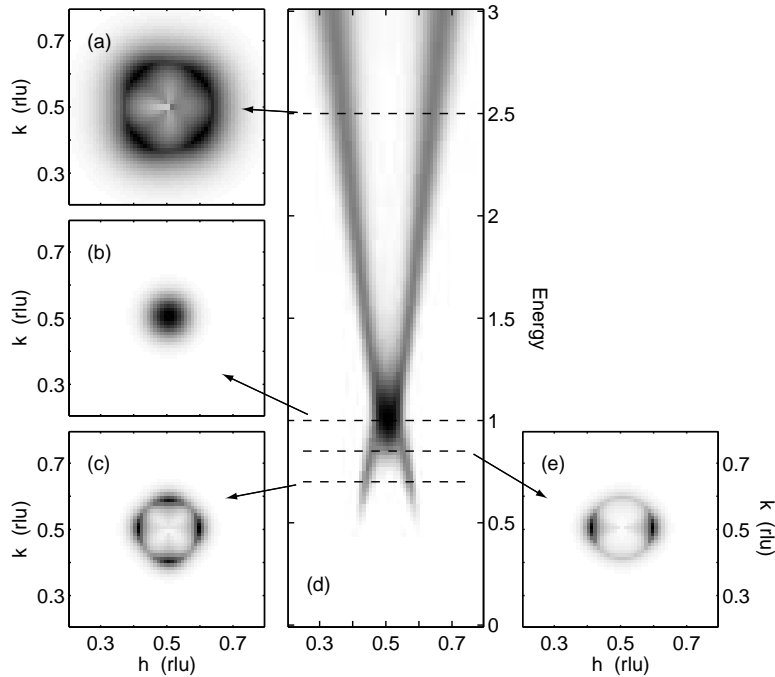
### 8.2.1 Dispersion

Most of the neutron scattering studies of cuprate superconductors have focused on two families:  $\text{La}_{2-x}\text{Sr}_x\text{CuO}_4$  and  $\text{YBa}_2\text{Cu}_3\text{O}_{6+x}$ . The simple reason for this is that these are the only compounds for which large crystals have been available. For quite some time it appeared that the magnetic spectra of these two families were distinct. In  $\text{La}_{2-x}\text{Sr}_x\text{CuO}_4$ , the distinctive feature was incommensurate scattering, studied at low energies ( $< 20$  meV) [11, 12, 13], whereas for  $\text{YBa}_2\text{Cu}_3\text{O}_{6+x}$  the attention was focused on the commensurate scattering (“41-meV” or “resonance” peak [14, 15, 16, 17, 18]) that grows in intensity (and shifts in energy [19]) as the temperature is cooled below  $T_c$ . A resonance peak was also detected in  $\text{Bi}_2\text{Sr}_2\text{CaCu}_2\text{O}_{8+\delta}$  [20, 21, 22] and in  $\text{Tl}_2\text{Ba}_2\text{CuO}_{6+\delta}$  [23]. Considerable theoretical attention has been directed towards the resonance peak and its significance (*e.g.*, see [24, 25, 26]). The fact that no strongly temperature-dependent excitation at  $\mathbf{Q}_{\text{AF}}$  was ever observed in  $\text{La}_{2-x}\text{Sr}_x\text{CuO}_4$  raised questions about the role of magnetic excitations the cuprate superconductivity.

While considerable emphasis has been placed on the resonance peak, it has been clear for quite some time that normal-state magnetic excitations in under-doped  $\text{YBa}_2\text{Cu}_3\text{O}_{6+x}$  extend over a large energy range [30, 31], comparable to that in the antiferromagnetic parent compound [32, 33]. The first clear signature that the excitations below the resonance are incommensurate, similar to the low-energy excitations in  $\text{La}_{2-x}\text{Sr}_x\text{CuO}_4$  [11, 13], was obtained by Mook *et al.* [34] for  $\text{YBa}_2\text{Cu}_3\text{O}_{6.6}$ . That these incommensurate excitations disperse inwards towards the resonance energy was demonstrated in  $\text{YBa}_2\text{Cu}_3\text{O}_{6.7}$  by Arai *et al.* [35] and in  $\text{YBa}_2\text{Cu}_3\text{O}_{6.85}$  by Bourges *et al.* [36]. More recent measurements have established a common picture of the dispersion [27, 37, 38, 28, 39].

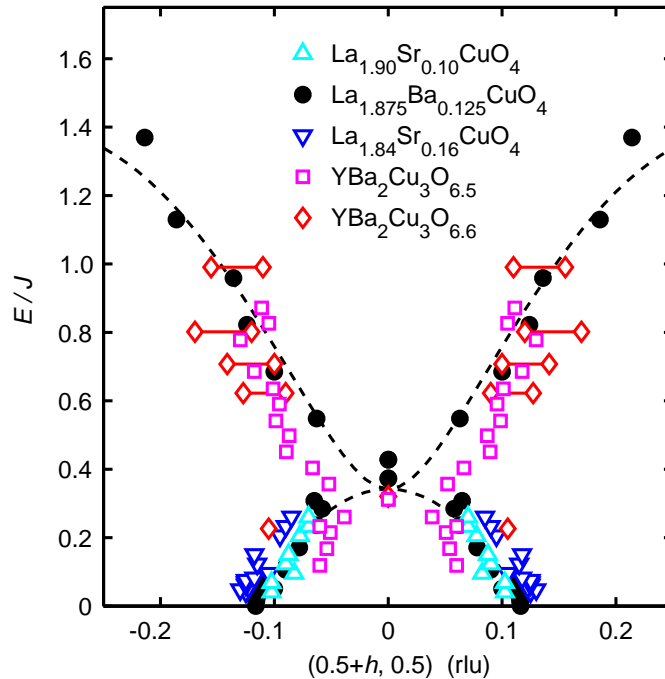
A schematic of the measured dispersion is shown in Fig. 8.2, with the energy normalized to that of the commensurate excitations,  $E_r$ . (Note that the distribution of intensity is not intended to accurately reflect experiment, especially in the superconducting state.) The figure also indicates the  $\mathbf{Q}$  dependence of magnetic scattering at fixed excitation energies. For  $E < E_r$ , measurements on crystallographically-twinned crystals indicate a four-fold intensity pattern, with maxima at incommensurate wave vectors displaced from  $\mathbf{Q}_{\text{AF}}$  along [100] and [010] directions. For  $E > E_r$ , Hayden *et al.* [27] infer for their  $\text{YBa}_2\text{Cu}_3\text{O}_{6.6}$  sample a four-fold structure that is rotated by  $45^\circ$  compared to low energies, whereas Stock *et al.* [28] find an isotropic ring of scattering for  $\text{YBa}_2\text{Cu}_3\text{O}_{6.5}$ . (These differences are minor compared to the overall level of agreement.) The spectrum with a finite spin gap is applicable to measurements below  $T_c$ ; the gap fills in above  $T_c$ , where it also becomes difficult to resolve any incommensurate features.

Fig. 8.3 shows a direct comparison of measurements on  $\text{La}_{2-x}\text{Sr}_x\text{CuO}_4$  [40] and under-doped  $\text{YBa}_2\text{Cu}_3\text{O}_{6+x}$  [27, 28], with energy scaled by the su-



**Fig. 8.2.** Schematic plots intended to represent neutron scattering measurements of  $\chi''(\mathbf{Q}, \omega)$  in superconducting  $\text{YBa}_2\text{Cu}_3\text{O}_{6+x}$  at  $T \ll T_c$ . Panels (a), (b), and (c) represent the distribution of scattering in reciprocal space about  $\mathbf{Q}_{\text{AF}}$  at relative energies indicated by the dashed lines in (d), for a twinned sample. (d)  $\chi''$  along  $\mathbf{Q} = (h, \frac{1}{2}, L)$  as a function of energy (normalized to the saddle-point energy, which is doping dependent). (a-d) modeled after [27, 28]. (e) Anisotropic distribution of scattering inferred for a detwinned, single-domain sample of  $\text{YBa}_2\text{Cu}_3\text{O}_{6.85}$ , after [29].

perexchange energy,  $J$  (see Table 8.1 in §8.3). Also included in the figure are results for  $\text{La}_{2-x}\text{Ba}_x\text{CuO}_4$  with  $x = \frac{1}{8}$  [41, 42], a compound of interest because of the occurrence of charge and spin stripe order [43] (to be discussed later) and a strongly suppressed  $T_c$ . At the lowest energies, the spin excitations rise out of incommensurate magnetic (two-dimensional) Bragg peaks. Besides the presence of Bragg peaks, the magnetic scattering differs from that of  $\text{YBa}_2\text{Cu}_3\text{O}_{6+x}$  in the absence of a spin gap. The results for optimally-doped  $\text{La}_{2-x}\text{Sr}_x\text{CuO}_4$ , with  $x = 0.16$ , interpolate between these cases, exhibiting the same inward dispersion of the excitations towards  $\mathbf{Q}_{\text{AF}}$  (measured up to 40 meV) and a spin gap of intermediate magnitude in the superconducting state [40]. The degree of similarity among the results shown in Fig. 8.3 is striking, and suggests that the magnetic dispersion spectrum may be universal in the cuprates [40, 44].



**Fig. 8.3.** Comparison of measured dispersions along  $\mathbf{Q}_{2D} = (0.5 + h, 0.5)$  in  $\text{La}_{2-x}\text{Sr}_x\text{CuO}_4$  with  $x = 0.10$  (up triangles) and  $0.16$  (down triangles) from Christensen *et al.* [40], in  $\text{La}_{1.875}\text{Ba}_{0.125}\text{CuO}_4$  (filled circles) from [42], and in  $\text{YBa}_2\text{Cu}_3\text{O}_{6+x}$  with  $x = 0.5$  (squares) from Stock *et al.* [28] and  $0.6$  (diamonds) from Hayden *et al.* [27]. The energy has been scaled by the superexchange energy  $J$  for the appropriate parent insulator as given in Table 8.1. For  $\text{YBa}_2\text{Cu}_3\text{O}_{6.6}$ , the data at higher energies were fit along the  $[1,1]$  direction; the doubled symbols with bars indicate two different ways of interpolating the results for the  $[1,0]$  direction. The upwardly-dispersing dashed curve corresponds to the result of Barnes and Riera [45] for a 2-leg spin ladder, with an effective superexchange of  $\sim \frac{2}{3}J$ ; the downward curve is a guide to the eye.

For optimally doped  $\text{YBa}_2\text{Cu}_3\text{O}_{6+x}$ , the measured dispersive excitations are restricted to a narrower energy window, as shown in Fig. 8.11. Nevertheless, excitations are observed to disperse both downward and upward from  $E_r$ , and the qualitative similarity with dispersions at lower doping is obvious.

Anisotropy of the magnetic scattering as a function of  $\mathbf{Q}_{2D}$  can be measured in specially detwinned samples of  $\text{YBa}_2\text{Cu}_3\text{O}_{6+x}$ , as the crystal structure has an anisotropy associated with the orientation of the CuO chains. (Note that it is a major experimental challenge to detwin samples of sufficient volume to allow a successful inelastic neutron scattering study.) An initial study of a partially detwinned sample of  $\text{YBa}_2\text{Cu}_3\text{O}_{6.6}$  by Mook *et*

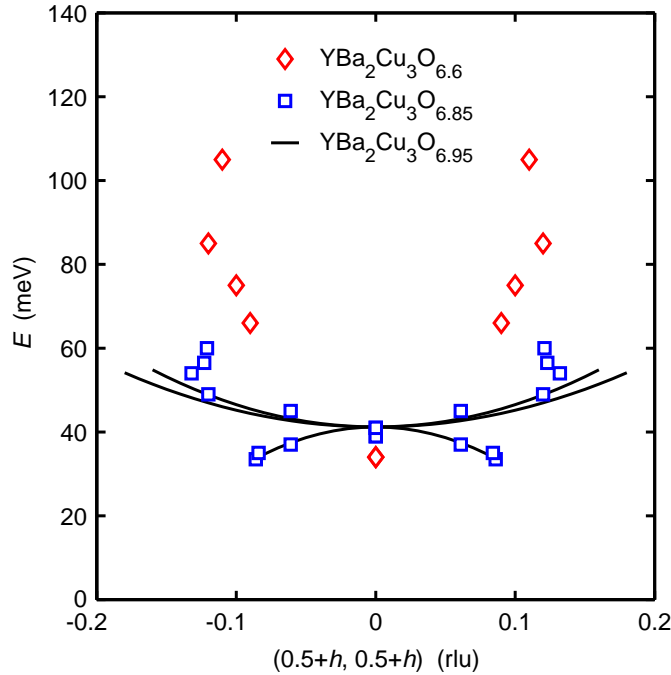


**Fig. 8.4.** Comparison of measured dispersions along  $\mathbf{Q}_{2D} = (0.5 + h, 0.5 + h)$  in the superconducting state of  $\text{YBa}_2\text{Cu}_3\text{O}_{6+x}$  with  $x = 0.6$  (diamonds) from Hayden *et al.* [27] and 0.85 (squares) from Pailhès *et al.* [37]. The solid lines represent the model dispersion (and variation in dispersion) compatible with measurements on  $\text{YBa}_2\text{Cu}_3\text{O}_{6.95}$  from Reznik *et al.* [38].

*al.* [46] demonstrated that, for the incommensurate scattering at an energy corresponding to 70% of the saddle point, the intensity is quite anisotropic, with maxima along the  $\mathbf{a}^*$  direction (perpendicular to the orientation of the CuO chains). A recent study of an array of highly detwinned crystals of  $\text{YBa}_2\text{Cu}_3\text{O}_{6.85}$  by Hinkov *et al.* [29] found substantial anisotropy in the peak scattered intensity for an energy of 85% of the saddle point, but also demonstrated that scattered intensity at that energy forms a circle about  $\mathbf{Q}_{AF}$  [see Fig. 8.2(e)]. Measurements on a partially-detwinned sample of  $\text{YBa}_2\text{Cu}_3\text{O}_{6.5}$  by Stock *et al.* [47, 28] suggest a strong anisotropy in the scattered intensity at  $0.36E_r$ , but essentially perfect isotropy for  $E > E_r$ .

### 8.2.2 Spin gap and “resonance” peak

For optimally-doped cuprates, the most dramatic change in the magnetic scattering with temperature is the opening of a spin gap, with redistribution of spectral weight from below to above the gap. A clear example of this has

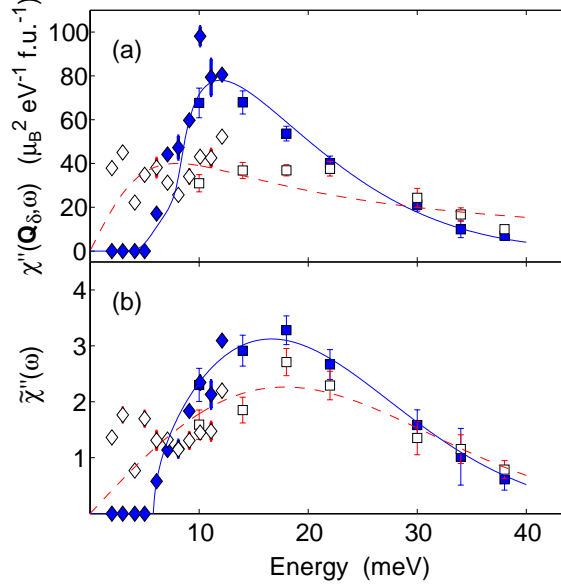


**Fig. 8.5.** (a) The fitted peak intensity of  $\chi''(\mathbf{Q}_\delta, \omega)$  (where  $\mathbf{Q}_\delta$  is the peak position) for  $\text{La}_{2-x}\text{Sr}_x\text{CuO}_4$  with  $x = 0.16$ . (b) The local susceptibility,  $\tilde{\chi}''(\omega)$ . Filled symbols:  $T < T_c$ ; open symbols:  $T > T_c$ . Results are a combination of data from time-of-flight measurements (squares) and triple-axis measurements (diamonds). Lines are guides to the eye. From Christensen *et al.* [40].

been presented recently by Christensen *et al.* [40] for  $\text{La}_{2-x}\text{Sr}_x\text{CuO}_4$  with  $x = 0.16$ ; their results are shown in Fig. 8.5. For the energy range shown, the scattering is incommensurate in  $\mathbf{Q}$ , with the dispersion indicated in Fig. 8.3. In the normal state, the amplitude of  $\chi''$  heads to zero only at  $\omega = 0$ ; in the superconducting state, weight is removed from below a spin gap energy of  $\Delta_s \approx 8$  meV, and shifted to energies just above  $\Delta_s$ . This is apparent both for the plot of the peak amplitude of  $\chi''$  in Fig. 8.5(a), and for the  $\mathbf{Q}$ -integrated  $\chi''$  in (b); within the experimental uncertainty, the spectral weight below 40 meV is conserved on cooling through  $T_c$  [40]. Another important feature of the spin gap is that its magnitude is independent of  $\mathbf{Q}$  [48]. This is of particular interest because it is inconsistent with a weak-coupling prediction of  $\chi''$  for a  $d$ -wave superconductor, assuming that the spin response comes from quasiparticles [49].

The behavior is similar near optimal doping in  $\text{YBa}_2\text{Cu}_3\text{O}_{6+x}$  [36, 37, 38, 17], with the difference being that the spin gap energy of  $\sim 33$  meV is much closer to  $E_r = 41$  meV. The strongest intensity enhancement below  $T_c$  occurs at  $E_r$ , where  $\chi''$  is peaked at  $\mathbf{Q}_{\text{AF}}$ ; however, there is also enhanced intensity at energies a bit below and above  $E_r$ , where  $\chi''$  is incommensurate [36, 37].



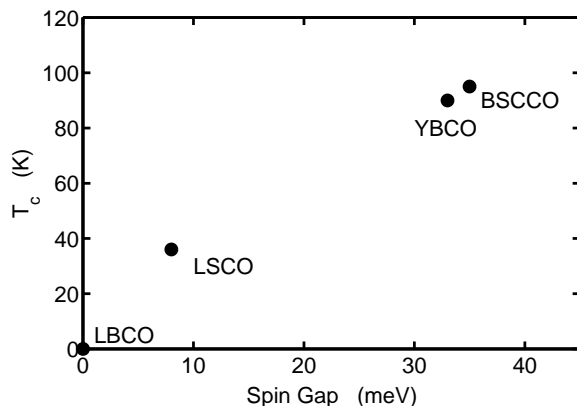


**Fig. 8.6.** Plot of  $T_c$  vs. spin-gap energy,  $\Delta_s$ , in cuprates near optimal doping. LSCO:  $\text{La}_{2-x}\text{Sr}_x\text{CuO}_4$  ( $x = 0.16$ ) from [40]; YBCO:  $\text{YBa}_2\text{Cu}_3\text{O}_{6.85}$  from [36]; BSCCO:  $\text{Bi}_2\text{Sr}_2\text{CaCu}_2\text{O}_{8+\delta}$  with  $\Delta_s$  estimated by scaling  $E_r$  with respect to  $\text{YBa}_2\text{Cu}_3\text{O}_{6+x}$ , from [20]; LBCO:  $\text{La}_{2-x}\text{Ba}_x\text{CuO}_4$  ( $x = \frac{1}{8}$ ) from [41].

The spin gap  $\Delta_s$  decreases and broadens with underdoping, so that the region over which  $\chi'' \approx 0$  is no more than a few meV for  $\text{YBa}_2\text{Cu}_3\text{O}_{6.5}$  [47, 30, 39].

Besides the temperature dependence, there is also a similar behavior of the enhanced intensity for these two cuprate families in response to an applied magnetic field. As the cuprates are type-II superconductors with a very small lower critical field, an applied magnetic field can enter a sample as an array of vortices. Dai *et al.* [50] showed that application of a magnetic field of 6.8 T along the  $c$  axis of  $\text{YBa}_2\text{Cu}_3\text{O}_{6.6}$  at  $T \ll T_c$  caused a reduction of the intensity at  $E_r$  by  $\sim 30\%$ . A study of  $\text{La}_{2-x}\text{Sr}_x\text{CuO}_4$  with  $x = 0.18$  found that application of a 10-T field along the  $c$ -axis caused a reduction of the intensity maximum at 9 meV of about 25% (with an increase in  $Q$  width) and a shift of some weight into the spin gap [51]. The field-induced increase of weight within the spin gap of  $\text{La}_{2-x}\text{Sr}_x\text{CuO}_4$  ( $x = 0.163$ ) was first observed by Lake *et al.* [52].

By focusing on  $\Delta_s$  rather than  $E_r$ , it is possible to identify a correlation between magnetic excitations and  $T_c$  that applies to a variety of cuprates. Figure 8.6 shows a plot of  $T_c$  as a function of the spin-gap energy for several different cuprates near optimal doping. This trend makes clear that the magnetic excitations are quite sensitive to the superconductivity, but, by itself, it does not resolve the issues of whether or how magnetic correlations may be involved in the pairing mechanism.

### 8.2.3 Discussion

From the results presented above, it now appears that there may be a universal magnetic excitation spectrum for the cuprates. On entering the supercon-

ducting state, a gap in the magnetic spectrum develops, with spectral weight redistributed from below to above the gap. The magnitude of the spin gap is correlated with  $T_c$ .

A long-standing question concerns the role of magnetic excitations in the mechanism of high-temperature superconductivity, and some varying perspectives are presented in later chapters of this book. An underlying issue concerns the nature of the magnetic excitations themselves. Given that  $\text{La}_{2-x}\text{Sr}_x\text{CuO}_4$  and  $\text{YBa}_2\text{Cu}_3\text{O}_{6+x}$  exhibit antiferromagnetically ordered phases when the hole-doping of the  $\text{CuO}_2$  planes goes to zero, one approach is to look for a connection between the magnetic correlations in the superconducting and in the correlated-insulator phases. On the other hand, the magnetic response of common metallic systems (such as chromium) is tied to the low-energy excitations of electrons from filled to empty states, across the Fermi surface. This motivates attempts to interpret the magnetic excitations in terms of electron-hole excitations. It is not clear that these contrasting approaches can be reconciled with one another [53], but, in any case, there are presently no consensual criteria for selecting one approach over another.

An experimentalist's approach is to consider the correlations in the superconducting cuprates in the context of related systems. Thus, in the following sections we consider experimental results for antiferromagnetic cuprates, other doped transition-metal-oxide systems, perturbations to the superconducting phase, and the doping dependence of the magnetic correlations in the superconductors. A comparison of theoretical approaches is better discussed within the full context of experimental results.

## 8.3 Antiferromagnetism in the parent insulators

### 8.3.1 Antiferromagnetic order

In the parent insulators, the magnetic moments of the copper atoms order in a 3D Néel structure. Powder neutron diffraction studies first demonstrated this for  $\text{La}_2\text{CuO}_4$  [2], and later for  $\text{YBa}_2\text{Cu}_3\text{O}_{6+x}$  [54]. The magnetic moments tend to lie nearly parallel to the  $\text{CuO}_2$  planes. The details of the magnetic structures are tied to the crystal structures, so we will have to consider these briefly.

The crystal structure of  $\text{La}_2\text{CuO}_4$  is presented in Fig. 8.7. The  $\text{CuO}_2$  planes are stacked in a body-centered fashion, so that the unit cell contains two layers. Below 550 K each  $\text{CuO}_6$  octahedron rotates about a [110] axis of the high-temperature tetragonal cell. Neighboring octahedra within a plane rotate in opposite directions, causing a doubling of the unit cell volume and a change to orthorhombic symmetry, with the  $\mathbf{a}_O$  and  $\mathbf{b}_O$  axes rotated by  $45^\circ$  with respect to the Cu-O bond directions. In the orthorhombic coordinates, the octahedral tilts are along the  $\mathbf{b}_O$  direction (but  $b_O > a_O$ , contrary to naive expectations).

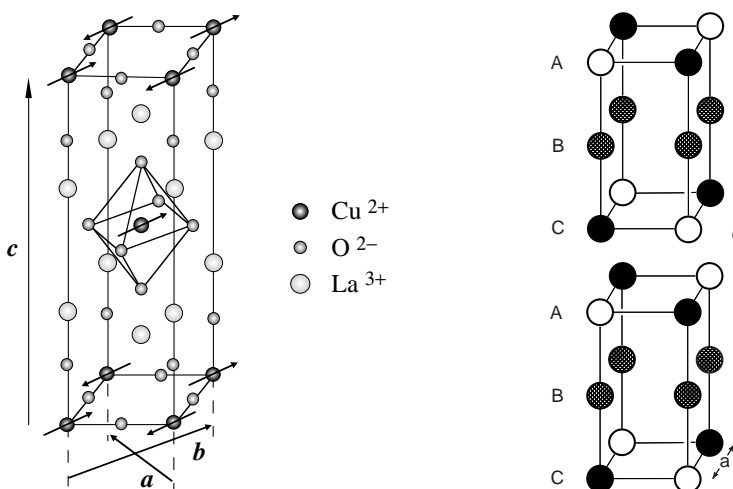


**Fig. 8.7.** Left: crystal structure of  $\text{La}_2\text{CuO}_4$ . Arrows indicate orientation of magnetic moments on Cu sites in the antiferromagnetic state. After Lee *et al.* [55]. Right: Magnetic structure of  $\text{YBa}_2\text{Cu}_3\text{O}_6$ . Circles: Cu atoms; lines: paths bridged by oxygen. Filled and empty circles represent  $\text{Cu}^{2+}$  sites with opposite spin orientations; hatched circles denote non-magnetic  $\text{Cu}^{1+}$  sites. After Tranquada *et al.* [56].

In the antiferromagnetic phase of  $\text{La}_2\text{CuO}_4$ , the spins point along the  $b_{\text{O}}$  axis, and they have the stacking sequence shown in Fig. 8.7 [2, 57]. As the octahedral tilts break the tetragonal symmetry of the planes, they allow spin-orbit effects, in the form of Dzyalozhinsky-Moriya (DM) antisymmetric exchange, to cause a slight canting of the spins along the  $c$  axis. This canting is in opposite directions for neighboring planes, resulting in no bulk moment, but a modest magnetic field can flip the spins in half of the planes, yielding a weakly ferromagnetic state [58]. The tendency to cant in the paramagnetic state above  $T_{\text{N}}$  leads to a ferromagnetic-like susceptibility at high temperatures and a cusp at  $T_{\text{N}}$  [59]. Studies of quasi-1D cuprates have made it clear that the DM (and additional) interactions are quite common [60]; however, the tetragonal  $\text{CuO}_2$  planes of other layered cuprate antiferromagnets cause the effects of the DM interaction to cancel out, so that there is no canting [61, 62].

In the early diffraction studies, the  $\text{La}_2\text{CuO}_4$  powder samples contained some excess oxygen and the first crystals had contamination from flux or the crucible, thus resulting in a reduced ordering temperature. (It is now known that excess oxygen, in sufficient quantity, can segregate to form superconducting phases [63].) It was eventually found that by properly annealing a crystal one can obtain a sample with  $T_{\text{N}} = 325$  K [64]. The ordered magnetic moment is also sensitive to impurity effects. In a study of single crystals with different annealing treatments, Yamada *et al.* [65] found that the ordered moment is

**Table 8.1.** Compilation of some neutron scattering results for a number of layered cuprate antiferromagnets.  $m_{\text{Cu}}$  is the average ordered moment per Cu atom at  $T \ll T_N$ . The superexchange energy  $J$  corresponds to the value obtained from the spin wave velocity after correction for the quantum-renormalization factor  $Z_c = 1.18$ . For crystal symmetry, O = orthorhombic, T = tetragonal.

Compound	$T_N$ (K)	$m_{\text{Cu}}$ ( $\mu_B$ )	$J$ (meV)	Crystal Symmetry	Layers per cell	Refs.
$\text{La}_2\text{CuO}_4$	325(2)	0.60(5)	146(4)	O	1	[65, 64, 68]
$\text{Sr}_2\text{CuO}_2\text{Cl}_2$	256(2)	0.34(4)	125(6)	T	1	[69, 70, 71]
$\text{Ca}_2\text{CuO}_2\text{Cl}_2$	247(5)	0.25(10)		T	1	[72]
$\text{Nd}_2\text{CuO}_4$	276(1)	0.46(5)	155(3)	T	1	[73, 74, 75, 76]
$\text{Pr}_2\text{CuO}_4$	284(1)	0.40(2)	130(13)	T	1	[77, 73]
$\text{YBa}_2\text{Cu}_3\text{O}_{6.1}$	410(1)	0.55(3)	106(7)	T	2	[78, 32]
$\text{TlBa}_2\text{YCu}_2\text{O}_7$	> 350	0.52(8)		T	2	[79]
$\text{Ca}_{0.85}\text{Sr}_{0.15}\text{CuO}_2$	537(5)	0.51(5)		T	$\infty$	[80]

correlated with  $T_N$ , with a maximum Cu moment of 0.60(5)  $\mu_B$  [apparently determined from the intensity of the (100) magnetic reflection alone].

The magnetic coupling between layers in  $\text{La}_2\text{CuO}_4$  is quite weak because each Cu sees two up spins and two down spins at nearly the same distance in a neighboring layer. The small orthorhombic distortion of the lattice removes any true frustration, resulting in a small but finite coupling. There are, however, several other cuprate antiferromagnets with a similar centered stacking of layers, but with tetragonal symmetry (see Table 8.1). Yildirim *et al.* [66] showed that the long-range order (including spin directions) can be understood when one takes into account zero-point spin fluctuations, together with the proper exchange anisotropies [67].

The parent compounds of the electron-doped superconductors,  $\text{Nd}_2\text{CuO}_4$  and  $\text{Pr}_2\text{CuO}_4$ , have somewhat more complicated magnetic structures. Nd moments and induced moments on Pr couple to the order in the  $\text{CuO}_2$  planes, resulting in noncollinear magnetic structures and spin reorientation transitions as a function of temperature; these are described in the review by Lynn and Skanthakumar [75]. The magnetic structures and transitions have been explained by Sachidanandam *et al.* [81] by taking account of the single-ion anisotropy and crystal-field effects for the rare-earth ions. Further discussion is given by Petitgrand *et al.* [82].

The crystal structure of  $\text{YBa}_2\text{Cu}_3\text{O}_{6+x}$  contains pairs of  $\text{CuO}_2$  layers (bilayers). There is also a third layer of Cu atoms, but in  $\text{YBa}_2\text{Cu}_3\text{O}_6$  these are non-magnetic  $\text{Cu}^{1+}$  ions. (Added oxygen goes into this layer, forming the  $\text{CuO}$  chains of  $\text{YBa}_2\text{Cu}_3\text{O}_7$ .) The magnetic structure of  $\text{YBa}_2\text{Cu}_3\text{O}_6$  is indicated in Fig. 8.7. Because of the relative antiferromagnetic ordering of the bilayers, together with a spacing that is not determined by symmetry, there is a structure factor for the magnetic Bragg peaks that depends on  $Q_z$ . This structure factor also affects the spin-wave intensities, as will be discussed.

It is not possible to determine the spin direction from zero-field diffraction measurements due to the tetragonal symmetry of the lattice and inevitable twinning of the magnetic domains. Nevertheless, Burlet *et al.* [83] were able to determine the spin direction by studying the impact of a magnetic field applied along a  $[1, -1, 0]$  direction of a  $\text{YBa}_2\text{Cu}_3\text{O}_{6.05}$  single crystal. They found that in zero field, the spins must lie along  $[100]$  or  $[010]$  directions (parallel to the Cu-O bonds), and that the applied field rotates them towards  $[110]$ . This result has been confirmed by electron-spin resonance studies of  $\text{YBa}_2\text{Cu}_3\text{O}_{6+x}$  with a small amount of Gd substituted for Y [84].

A complication in studies of magnetic order involving some of the first crystals of  $\text{YBa}_2\text{Cu}_3\text{O}_{6+x}$  arose from inadvertent partial substitution of Al ions onto the Cu(1) (“chain”) site. The Al presumably came from the use of crucibles made of  $\text{Al}_2\text{O}_3$ . Kadowaki *et al.* [85], performing one of the first single-crystal diffraction studies on a  $\text{YBa}_2\text{Cu}_3\text{O}_{6+x}$  sample with  $T_N$  of 405 K, found that below 40 K a new set of superlattice peaks appeared, indicating a doubling of the magnetic unit cell along the  $c$  axis. It was later demonstrated convincingly, by comparing pure and Al-doped crystals, that the low-temperature doubling of the magnetic period only occurs in crystals with Al [78, 86]. A model explaining how the presence of Al on Cu chain sites can change the magnetic order was developed by Andersen and Uimin [87].

To evaluate the ordered magnetic moment, it is necessary to have knowledge of the magnetic form factor. In all of the early studies of antiferromagnetic order in cuprates it was assumed that the spin-density on a Cu ion is spherical; however, this assumption is far from being correct. The magnetic moment results from the half-filled  $3d_{x^2-y^2}$  orbital, which deviates substantially from sphericity. The proper, anisotropic form factor was identified by Shamoto *et al.* [88] and shown to give an improved description of magnetic Bragg intensities for  $\text{YBa}_2\text{Cu}_3\text{O}_{6.15}$ . An even better measurement of magnetic Bragg peaks was done on small crystal of  $\text{YBa}_2\text{Cu}_3\text{O}_{6.10}$  by Casalta *et al.* [78]. They obtained a Cu moment of  $0.55(3) \mu_B$ . Use of the proper form factor is important for properly evaluating the magnetic moment, as there is always a gap between  $Q = 0$  (where the magnitude of the form factor is defined to be 1) and the  $Q$  value of the first magnetic Bragg peak. It does not appear that anyone has gone back to reevaluate the magnetic diffraction data on other cuprates, such as  $\text{La}_2\text{CuO}_4$  or  $\text{Sr}_2\text{CuO}_2\text{Cl}_2$  using the anisotropic form factor.

The maximum observed Cu moments are consistent with a large reduction due to zero-point spin fluctuations as predicted by spin-wave theory. The moment  $m$  is equal to  $g\langle S \rangle \mu_B$ , where a typical value of the gyromagnetic ratio  $g$  is 2.1. Without zero-point fluctuations, one would expect  $m \approx 1.1 \mu_B$ . Linear spin-wave theory predicts  $\langle S \rangle = 0.303$  [89], giving  $m \approx 0.64 \mu_B$ , a bit more than the largest observed moments. Further reductions can occur due to hybridization effects [90, 91].

The ordered moments of the oxy-chlorides listed in Table 8.1 seem surprisingly small. While this might be due to hybridization effects, it is interesting to note that there is a correlation between  $m_{\text{Cu}}$  and  $T_N$  for the first five anti-

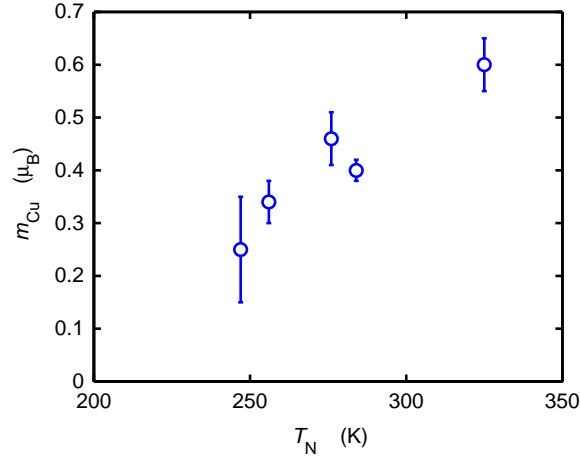


**Fig. 8.8.** Ordered magnetic moment per Cu atom vs.  $T_N$  for the first five compounds in Table 8.1, all of which have a similar body-centered stacking of  $\text{CuO}_2$  layers.

ferromagnets in the table, which all share a similar body-centered stacking of the  $\text{CuO}_2$  planes. The correlation is illustrated in Fig. 8.8. The ratio  $T_N/J$  is expected to be sensitive to the interlayer exchange  $J'$  [92], and  $J'$  varies substantially among these compounds; however, I am not aware of any predicted dependence of  $m_{\text{Cu}}$  on  $J'$ . A correlation between  $m_{\text{Cu}}$  and  $T_N/J$  has been reported for quasi-1D antiferromagnets, but such a correlation is expected in that case [93].

### 8.3.2 Spin waves

The starting point for considering magnetic interactions in the cuprates is the Heisenberg hamiltonian:

$$H = J \sum_{\langle i,j \rangle} \mathbf{S}_i \cdot \mathbf{S}_j, \quad (8.5)$$

where  $\langle i,j \rangle$  denotes all nearest-neighbor pairs, each included once. This hamiltonian can be derived in second-order perturbation from a Hubbard model for a single, half-filled band of electrons. Such a model includes a nearest-neighbor hopping energy  $t$  and the Coulomb repulsion energy  $U$  for two electrons on the same site; in terms of these parameters,  $J = 4t^2/U$  [94]. Spin-wave theory can be applied to the Heisenberg hamiltonian to calculate the dispersion of spin fluctuations about  $\mathbf{Q}_{\text{AF}}$  [95]. At low energies the spin waves disperse linearly with  $\mathbf{q} = \mathbf{Q} - \mathbf{Q}_{\text{AF}}$  (see Fig. 8.9), having a velocity  $c = \sqrt{8}SZ_cJa/\hbar$ , where  $Z_c \approx 1.18$  [96] is a quantum-renormalization factor. Thus, by measuring the spin-wave velocity, one can determine  $J$ .

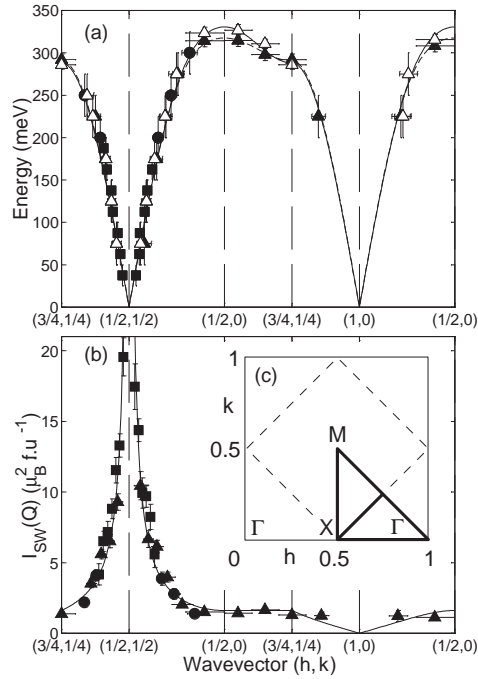


**Fig. 8.9.** (a) Spin-wave dispersion in  $\text{La}_2\text{CuO}_4$  along high-symmetry directions in the 2D Brillouin zone, as indicated in (c);  $T = 10$  K (295 K): open (filled) symbols. Solid (dashed) line is a fit to the 10-K (295-K) data. (b) Spin-wave intensity vs. wave vector. Line is prediction of linear spin-wave theory. From Coldea *et al.* [68].

Spin-wave measurements have been performed for a number of cuprates, and some results for  $J$  are listed in Table 8.1. (Complementary measurements of  $J$  can be obtained by two-magnon Raman scattering [97].) To calculate the values of  $J$  from spectroscopically determined parameters, one must consider at least a 3-band Hubbard model [98]. Recent *ab initio* cluster calculations [99, 100] have been able to achieve reasonable agreement with experiment. While the magnitude of  $J$  in layered cuprates is rather large, it is not extreme; a value of  $J = 226(12)$  meV has been measured for Cu-O chains in  $\text{SrCuO}_2$  [101].

To describe the experimental dispersion curves in greater detail, one must add more terms to the spin hamiltonian. For example, in a *tour de force* experiment, Coldea *et al.* [68] have measured the dispersion of spin waves in  $\text{La}_2\text{CuO}_4$  along high-symmetry directions of the 2D Brillouin zone, as shown in Fig. 8.9. The observed dispersion along the zone boundary, between  $(\frac{1}{2}, 0)$  and  $(\frac{3}{4}, \frac{1}{4})$ , is not predicted by the simple Heisenberg model. To describe this, they consider the additional terms that appear when the perturbation expansion for the single-band Hubbard model is extended to fourth order. The

most important new term involves 4-spin cyclic exchange about a plaquette of four Cu sites [102, 103, 104]. Coldea and coworkers were able to fit the data quite well with the added parameters [see lines through data points in Fig. 8.9(a)], obtaining, at 10 K,  $J = 146(4)$  meV and a cyclic exchange energy  $J_c = 61(8)$  meV [68]. (Superexchange terms coupling sites separated by two hops are finite but negligible.)

If, instead of expanding to higher order, one extends the Hubbard model to include hopping between next-nearest-neighbor Cu sites, one can calculate a superexchange term  $J'$  between next-nearest neighbors that is on the order of 10% of  $J$  [105, 106]. It turns out, however, that fitting the measured dispersion with only  $J$  and  $J'$  requires that  $J'$  correspond to a ferromagnetic interaction [68], which is inconsistent with the model predictions.

In  $\text{YBa}_2\text{Cu}_3\text{O}_{6+x}$ , the effective exchange coupling between Cu moments in nearest-neighbor layers is substantial. Its effect is to split the spin waves into acoustic and optic branches, having odd and even symmetry, respectively, with respect to the bilayers. The structure factors for these excitations are [107]

$$g_{\text{ac}} = \sin(\pi z l), \quad (8.6)$$

$$g_{\text{op}} = \cos(\pi z l), \quad (8.7)$$

where  $z = d_{\text{Cu-Cu}}/c$  is the relative spacing between Cu moments along the  $c$  axis within a bilayer ( $d_{\text{Cu-Cu}} \approx 3.285$  Å [108]); the intensity of the spin-wave scattering is proportional to  $g^2$ . An example of the intensity modulation due to the acoustic-mode structure factor in the antiferromagnetic state is indicated by the filled circles in Fig. 8.10.

The energy gap for the optical magnons has been measured to be approximately 70 meV [33, 32]. Experimental results for the spin wave dispersion and the spectral weight are shown in Fig. 8.11. The magnitude of the gap indicates that the intra-bilayer exchange is 11(2) meV [33, 32].

At low energies, there are other terms that need to be considered. There need to be anisotropies, with associated spin-wave gaps, in order to fix the spin direction; however, an atom with  $S = \frac{1}{2}$  cannot have single-ion anisotropy. Instead, the anisotropy is associated with the nearest-neighbor superexchange interaction. Consider a pair of nearest-neighbor spins,  $\mathbf{S}_i$  and  $\mathbf{S}_j$ , within a  $\text{CuO}_2$  plane, with each site having tetragonal symmetry. The Heisenberg Hamiltonian for this pair can be written

$$H_{\text{pair}} = J_{\parallel} S_i^{\parallel} S_j^{\parallel} + J_{\perp} S_i^{\perp} S_j^{\perp} + J_z S_i^z S_j^z, \quad (8.8)$$

where  $\parallel$  and  $\perp$  denote directions parallel and perpendicular to the bond within the plane, and  $z$  is the out-of-plane direction. Yildirim *et al.* [67] showed that the anisotropy can be explained by taking into account both the spin-orbit and Coulomb exchange interactions. To discuss the anisotropies, it is convenient to define the quantities  $\Delta J \equiv J_{\text{av}} - J_z$ , where  $J_{\text{av}} \equiv (J_{\parallel} + J_{\perp})/2$ , and  $\delta J_{\text{in}} \equiv J_{\parallel} - J_{\perp}$  [66]. For the cuprates,  $J_{\text{av}} \gg \Delta J > \delta J_{\text{in}} > 0$ . The out-of-plane



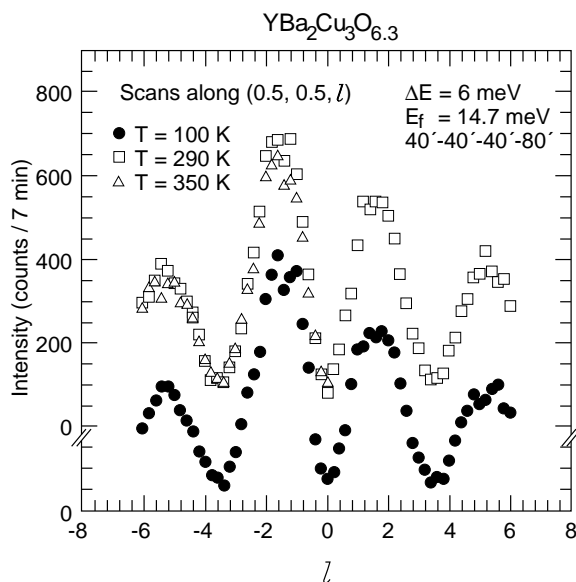


**Fig. 8.10.** Scans along the quasi-2D antiferromagnetic scattering rod  $\mathbf{Q} = (\frac{1}{2}, \frac{1}{2}, l)$  at a fixed energy transfer of 6 meV for a crystal of  $\text{YBa}_2\text{Cu}_3\text{O}_{6.3}$  with  $T_N = 260(5)$  K. The sinusoidal modulation is due to the inelastic structure factor. The asymmetry in the scattering as a function of  $l$  is an effect due to the experimental resolution function [9]; the decrease in intensity at large  $|l|$  is due to the magnetic form factor. After Tranquada *et al.* [107].

anisotropy,  $\alpha_{XY} = \Delta J / J_{\text{av}}$ , causes the spins to lie, on average, in the  $x$ - $y$  plane, and results in a spin-wave gap for out-of-plane fluctuations. The in-plane anisotropy  $\delta J_{\text{in}} / J_{\text{av}}$ , contributing through the quantum zero-point energy [66, 109], tends to favor alignment of the spins parallel to a bond direction, and causes the in-plane spin-wave mode to have a gap. The effective coupling between planes (which can involve contributions from several interactions [66]) leads to (weak) dispersion along  $Q_z$ .

For stoichiometric  $\text{La}_2\text{CuO}_4$ , the out-of-plane spin gap is 5.5(5) meV, corresponding to  $\alpha_{XY} = 1.5 \times 10^{-4}$  [110]. The in-plane gap of 2.8(5) meV has a contribution from anisotropic exchange of the Dzyaloshinsky-Moriya type [111, 112], as well as from  $\delta J_{\text{in}}$ . No dispersion along  $Q_z$  has been reported.

For antiferromagnetic  $\text{YBa}_2\text{Cu}_3\text{O}_{6+x}$ , an out-of-plane gap of about 5 meV has been observed [107, 113, 114], indicating an easy-plane anisotropy similar to that in  $\text{La}_2\text{CuO}_4$ . No in-plane gap has been resolved; however, the in-plane mode shows a dispersion of about 3 meV along  $Q_z$  [107, 113, 114]. The latter dispersion is controlled by the effective exchange between Cu moments in neighboring bilayers through the nonmagnetic Cu(1) sites, which is on the order of  $10^{-4}J$ .

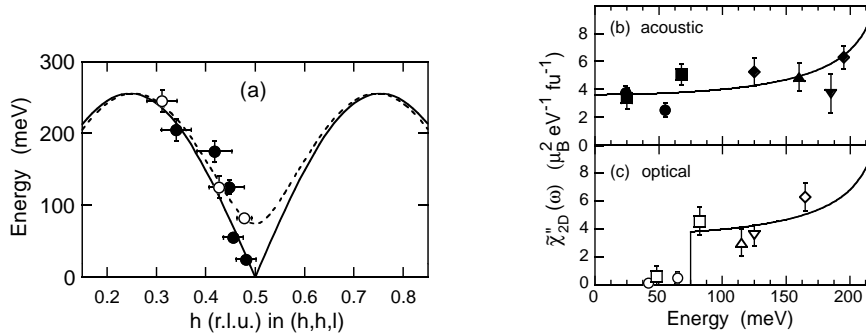


**Fig. 8.11.** Experimental results for  $\text{YBa}_2\text{Cu}_3\text{O}_{6.15}$ . (a) Dispersion of acoustic (filled symbols, solid line) and optic (open symbols, dashed line) spin-wave modes. (b)  $\mathbf{Q}$ -integrated dynamic susceptibility,  $\tilde{\chi}''(\omega)$  for the acoustic, and (c) optic modes. After Hayden *et al.* [32].

### 8.3.3 Spin dynamics at $T > T_N$

That strong 2D spin correlations survive in the  $\text{CuO}_2$  planes for  $T > T_N$  initially came as a surprise [115]. Such behavior was certainly uncommon at that point. Detailed studies have since been performed measuring the instantaneous spin correlation length  $\xi$  as a function of temperature in  $\text{La}_2\text{CuO}_4$  [116] and in  $\text{Sr}_2\text{CuO}_2\text{Cl}_2$  [117, 70]. The correlation length is obtained using an experimental trick to integrate the inelastic scattering over excitation energy, and using the formula

$$S(\mathbf{q}_{2D}) = \int d\omega S(\mathbf{q}_{2D}, \omega) = \frac{S(0)}{1 + q_{2D}^2 \xi^2}. \quad (8.9)$$

Here,  $\mathbf{q}_{2D}$  is the momentum-transfer component parallel to the planes, and the scattering is assumed to be independent of momentum transfer perpendicular to the planes. (The experimental energy integration is imperfect, but, by proper choice of incident neutron energy, does capture most of the critical scattering.)

To theoretically analyze the behavior of the correlation length, Chakravarty, Halperin, and Nelson [118] evaluated the 2D quantum nonlinear  $\sigma$  model using renormalization group techniques; their results were later extended to a higher-order approximation by Hasenfratz and Niedermayer [119]. The essential result is that

$$\xi/a \sim e^{2\pi\rho_s/T}, \quad (8.10)$$

where the spin stiffness  $\rho_s$  is proportional to  $J$  (see [116] for a thorough discussion). The experimental results are in excellent agreement with theory, with essentially no adjustable parameters. The unusual feature of  $\xi(T)$  is the exponential, rather than algebraic, dependence on temperature; nevertheless,

note that it is consistent with achieving long-range order at  $T = 0$ . The robustness of the experimentally-observed spin correlations is due to the large value of  $J$ , comparable to 1500 K, and the weak interlayer exchange,  $J'$ . The 3D ordering temperature can be estimated as [120]

$$kT_N \approx J' \left( \frac{m}{m_0} \right)^2 \left( \frac{\xi}{a} \right)^2, \quad (8.11)$$

where  $m/m_0 = 0.6$  is the reduction of the ordered moment due to quantum fluctuations. Because of the small  $J'$ , the correlation length can reach the order of  $100a$  before ordering occurs [116].

Although  $\text{Sr}_2\text{CuO}_2\text{Cl}_2$  has essentially the same structure as  $\text{La}_2\text{CuO}_4$ , its tetragonal symmetry leads one to expect, classically, that the net interlayer exchange should be zero; however, an analysis by Yildirim *et al.* [66] has shown that a finite interaction of appropriate size results when quantum zero-point energy is taken into account. Because of its relatively low  $T_N$  of 257 K, it has been possible to detect in  $\text{Sr}_2\text{CuO}_2\text{Cl}_2$  a crossover to XY-like behavior about 30 K above  $T_N$ , as reported in a  $^{35}\text{Cl}$  NMR study [121]. This behavior results from the small easy-plane exchange anisotropy common to the layered cuprates [122]. Using neutrons to study the same material, it was possible to show that the characteristic fluctuation rate in the paramagnetic state follows the behavior  $\Gamma = \omega_0 \sim \xi^{-z}$  with  $z = 1.0(1)$  [123], consistent with dynamic scaling theory for the 2D Heisenberg antiferromagnet.[124]

There has been less work done on the paramagnetic phase of  $\text{YBa}_2\text{Cu}_3\text{O}_{6+x}$ , as the inelastic structure factor, Eq. 8.6, complicates the experimental trick for energy integration. There are also complications to studying  $\text{YBa}_2\text{Cu}_3\text{O}_{6+x}$  samples at elevated temperatures, as oxygen can easily diffuse into and out of crystals as one heats much above room temperature. In any case, Fig. 8.10 shows that the bilayers remain correlated at  $T > T_N$  [107].

## 8.4 Destruction of antiferromagnetic order by hole doping

The long-range antiferromagnetic order of  $\text{La}_2\text{CuO}_4$  is completely destroyed when 2% of Sr (measured relative to Cu concentration) is doped into the system [125]. Adding holes effectively reduces the number of Cu spins, so one might consider whether the reduction of order is due to dilution of the magnetic lattice. For comparison, an extensive study of magnetic dilution has been performed by Vajk *et al.* [126] on  $\text{La}_2\text{Cu}_{1-z}(\text{Zn},\text{Mg})_z\text{O}_4$ , where Cu is substituted by nonmagnetic Zn and/or Mg. They found that long-range antiferromagnetic order was lost at the classical 2D percolation limit of  $z \approx 41\%$ . Thus, holes destroy magnetic order an order of magnitude more rapidly than does simple magnetic dilution.

The reduction of the Néel temperature at small but finite doping is accompanied by a strong depression of the antiferromagnetic Bragg intensities,

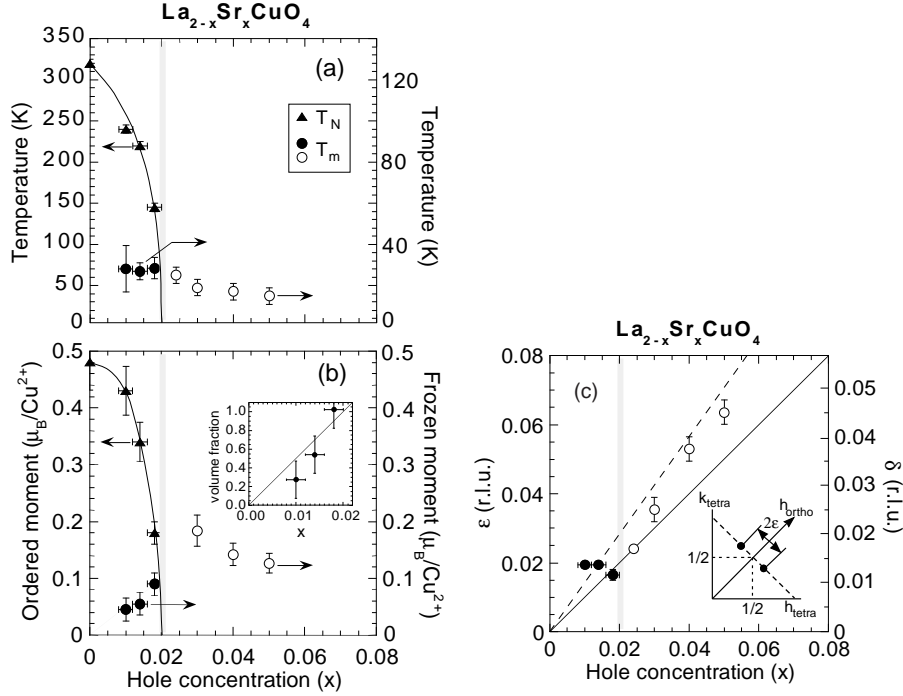


**Fig. 8.12.** Results for lightly-doped  $\text{La}_{2-x}\text{Sr}_x\text{CuO}_4$ . (a) Magnetic transition temperatures for commensurate (triangles) and incommensurate (circles) order vs. hole concentration. (b) Commensurate ordered moment at  $T = 30$  K and incommensurate frozen moment at  $T = 4$  K vs. hole concentration. Inset shows estimated volume fraction of incommensurate phase. (c) Variation of the incommensurability  $\epsilon$  vs. hole concentration;  $\delta = \epsilon/\sqrt{2}$ . Solid and broken lines correspond to  $\epsilon = x$  and  $\delta = x$ , respectively. Inset shows the positions of the incommensurate superlattice peaks in reciprocal space. After Matsuda *et al.* [127], including results from [128, 129, 130, 131].

together with an anomalous loss of intensity at  $T < 30$  K [127]. Matsuda *et al.* [127] showed recently that the latter behavior is correlated with the onset of incommensurate magnetic diffuse scattering below 30 K. In tetragonal coordinates, this scattering is peaked at  $(\frac{1}{2}, \frac{1}{2}, 0) \pm \frac{1}{\sqrt{2}}(\epsilon, \epsilon, 0)$ . To be more accurate, it is necessary to note that the crystal structure is actually orthorhombic, with the unit-cell axes rotated by  $45^\circ$ ; the magnetic modulation is uniquely oriented along the  $b_0^*$  direction [see inset of Fig. 8.12(c)].

The doping dependence of the transition temperature, ordered moments, and incommensurability are shown in Fig. 8.12. The facts that (a) the volume fraction of the incommensurate phase grows with  $x$  for  $x \leq 0.02$  [inset of Fig. 8.12(b)] and (b) the incommensurability does not change for  $x \leq 0.02$

strongly suggest that an electronic phase separation occurs [127]. Thus, it appears that commensurate antiferromagnetic order is not compatible with hole doping. The disordered potential due to the Sr dopants may be responsible for the finite range of doping over which the Néel state appears to survive. The diagonally-modulated, incommensurate spin-density-wave phase induced by doping survives up to the onset of superconductivity at  $x \approx 0.06$  [131], and it corresponds to what was originally characterized as the “spin-glass” phase, based on bulk susceptibility studies [132, 133].

Further evidence for electronic phase separation comes from studies of oxygen-doped  $\text{La}_2\text{CuO}_{4+\delta}$  (for a review, see [134]). The oxygen interstitials are mobile, in contrast to the quenched disorder of Sr substitution, and so they can move to screen discrete electronic phases. For  $\delta < 0.06$ , a temperature-dependent phase separation is observed between an oxygen-poor antiferromagnetic phase and an oxygen-rich superconducting phase [135, 136]; further miscibility gaps are observed between superconducting phases at higher oxygen content [63]. A sample with  $\delta \approx 0.05$  and quenched disorder (due to electrochemical oxygenation in molten salt) exhibited reduced Néel and superconducting transition temperatures [137]. The interesting feature in this case was the observation of a decrease in the antiferromagnetic order with the onset of the superconductivity, suggesting a competition between the two phases.

In  $\text{YBa}_2\text{Cu}_3\text{O}_{6+x}$  the situation is somewhat more complicated, as the doping of the planes is coupled to the tetragonal-orthorhombic (T-O) transition [138, 139, 140] that occurs in the vicinity of  $x = 0.3$ – $0.4$ , depending on the degree of annealing. In the tetragonal phase, an isolated oxygen atom entering the “chain” layer simply converts neighboring Cu(1) sites from  $\text{Cu}^{1+}$  to  $\text{Cu}^{2+}$ ; holes are created when chain segments form [54, 141]. The transfer of holes from the chains to the planes must be screened by displacements in the Ba-O layer that sits between, and a large jump in this screening occurs at the T-O transition [138, 139, 140]. Thus, one tends to find a discontinuous jump from a very small planar hole density in the antiferromagnetic phase just below the T-O transition to a significant density ( $\sim 0.05$  holes/Cu) just above.

Antiferromagnetic order has been observed throughout the tetragonal phase of  $\text{YBa}_2\text{Cu}_3\text{O}_{6+x}$ , with  $T_N$  decreasing rapidly as the T-O transition (at  $x \approx 0.4$ ) is approached [54, 142]. A study of a set of carefully annealed powder samples, for which the T-O transition occurred at  $x \approx 0.2$ , indicated antiferromagnetic order in the orthorhombic phase at  $x = 0.22$  and  $0.24$  with  $T_N = 50(15)$  K and  $20(10)$  K, respectively. For tetragonal crystals with  $x \sim 0.3$ , a drop in the antiferromagnetic Bragg intensity has been observed below  $\approx 30$  K [107, 142]; as the Bragg intensity decreased, an increase in diffuse intensity along the 2D antiferromagnetic rod (with an acoustic bilayer structure factor) was found. This latter behavior might be related to the apparent phase separation in  $\text{La}_{2-x}\text{Sr}_x\text{CuO}_4$  with  $x < 0.02$  [127] discussed above.

The best study of a single-crystal sample just on the orthorhombic side of the T-O boundary is on  $\text{YBa}_2\text{Cu}_3\text{O}_{6.35}$ , a sample with  $T_c = 18$  K [143].

Quasielastic diffuse scattering is observed at the antiferromagnetic superlattice positions. The peak intensity of this central mode grows on cooling below  $\sim 30$  K, but the energy width decreases below  $T_c$ . These results indicate there is no coexistence of long-range antiferromagnetic order in the superconducting phase. The spin-spin correlation length is short ( $\sim 8$  unit cells), suggesting segregation of hole-poor and hole-rich regions [143].

A possibly-related response to doping is observed in the bilayer system  $\text{La}_{2-x}(\text{Sr,Ca})_x\text{CaCu}_2\text{O}_{6+\delta}$ . Studies of crystals with  $x = 0.1\text{--}0.2$  reveal commensurate short-range antiferromagnetic order that survives to temperatures  $> 100$  K [144, 145], despite evidence from optical conductivity measurements for a substantial hole density in the  $\text{CuO}_2$  planes [146]. Thus, there seems to be a local phase separation between hole-rich regions and antiferromagnetic clusters having an in-plane diameter on the order of 10 lattice spacings.

## 8.5 Stripe order and other competing states

### 8.5.1 Charge and spin stripe order in nickelates

To understand cuprates, it seems sensible to consider the behavior of closely related model systems. One such system is  $\text{La}_{2-x}\text{Sr}_x\text{NiO}_{4+\delta}$ , a material that is isostructural with  $\text{La}_{2-x}\text{Sr}_x\text{CuO}_4$ . It is obtained by replacing  $S = \frac{1}{2}$   $\text{Cu}^{2+}$  ions ( $Z = 29$ ) with  $S = 1$   $\text{Ni}^{2+}$  ions ( $Z = 28$ ). One might consider the nickelates to be uninteresting as they are neither superconducting nor metallic (for  $x < 0.9$ ) [147, 148]; however, the insulating behavior is inconsistent with the predictions of band theory, and it is important to understand why.

Pure  $\text{La}_2\text{NiO}_4$  is an antiferromagnetic insulator [155] that is easily doped with excess oxygen, as well as by Sr substitution for La [134]. Doping the  $\text{NiO}_2$  planes with holes reduces  $T_N$  more gradually than in the cuprates [156]. It is necessary to dope to a hole concentration of  $n_h = x + 2\delta \sim 0.2$  before the commensurate antiferromagnetic order is replaced by stripe order [156, 151, 152]. Figure 8.13(a) shows a schematic of diagonal stripe order appropriate for  $n_h \approx 1/4$ . The charge stripes, with a hole filling of one per Ni site, act as antiphase domain walls for the magnetic order, so that the magnetic period is twice that of the charge order. The nature of the stripe order has been deduced from the positions and intensities of the superlattice peaks [134, 157]. The characteristic wave vector for spin order is  $\mathbf{q}_{\text{so}} = \mathbf{Q}_{\text{AF}} \pm \frac{1}{\sqrt{2}}(\epsilon, \epsilon, 0)$  and that for charge order is  $\mathbf{q}_{\text{co}} = \frac{1}{\sqrt{2}}(2\epsilon, 2\epsilon, 0) + (0, 0, 1)$ . When the symmetry of the average lattice does not pick a unique orientation, modulations rotated by  $90^\circ$  will also be present in separate domains. The fact that diagonal stripe order has a unique modulation direction within each domain has been confirmed by electron diffraction [158]. Evidence for significant charge modulation has also been provided by nuclear magnetic resonance studies [159, 160]. The charge-ordering transition is always observed to occur at a higher temperature

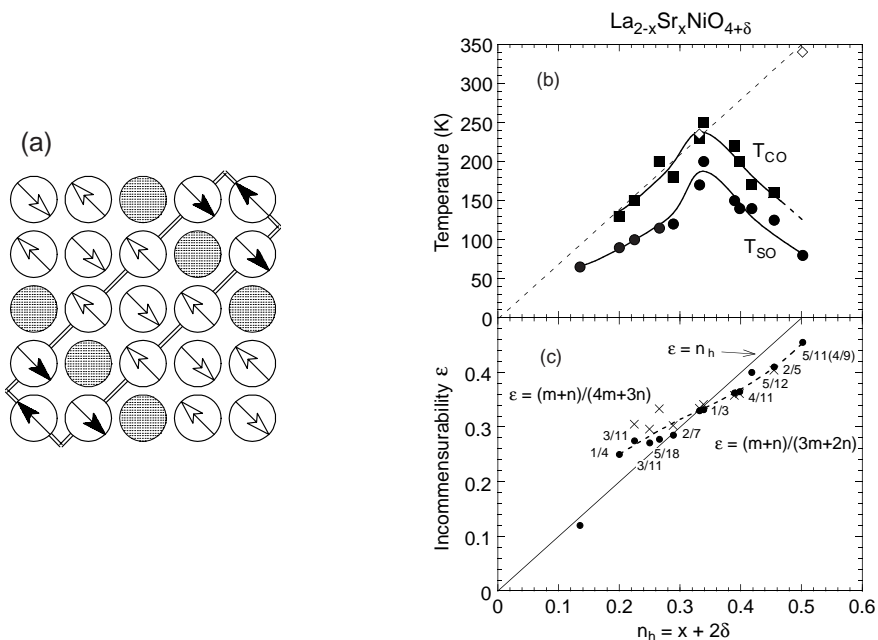


**Fig. 8.13.** (a) Cartoon of diagonal stripe order in an  $\text{NiO}_2$  plane (only Ni sites indicated) for  $n_h \approx 1/4$ . Magnetic unit cell is indicated by double lines, shaded circles indicate charge stripes with a hole density of one per Ni site. (b) Transition temperatures for charge order,  $T_{\text{CO}}$  (squares), and spin order,  $T_{\text{SO}}$  (circles), measured by neutron diffraction. Open diamonds: transition temperatures from transport measurements [149]. (c) Incommensurability vs.  $n_h$ . Circles (crosses) results at low temperature (high temperature, near  $T_{\text{SO}}$ ). Fraction labels are approximate long-period commensurabilities. (b) and (c) after Yoshizawa *et al.* [150], including results from [151, 152, 153, 154].

than the spin ordering, as shown in Fig. 8.13(b), with the highest ordering temperatures occurring for  $x = 1/3$  [149, 161].

The magnetic incommensurability  $\epsilon$ , is inversely proportional to the period of the magnetic modulation. It increases steadily with doping, as shown in Fig. 8.13(c), staying close to the line  $\epsilon = n_h$ , indicating that the hole-density within the charge stripes remains roughly constant but the stripe spacing decreases with doping. For a given sample, the incommensurability changes with temperature, tending towards  $\epsilon = 1/3$  as  $T \rightarrow T_{\text{CO}}$  [162]. In a sample with ordered oxygen interstitials,  $\epsilon$  has been observed to pass through lock-in plateaus on warming, indicating a significant coupling to the lattice [154].

The impact of hole-doping on the magnetic interactions has been determined from measurements of the spin-wave dispersions for crystals with  $x \approx 1/3$  [163, 164, 165]. Analysis shows that the superexchange  $J$  within an antiferromagnetic region is  $27.5(4)$  meV [165], which is only a modest reduc-

tion compared to  $J = 31(1)$  meV in undoped  $\text{La}_2\text{NiO}_4$  [166]. The effective coupling across a charge stripe is found to be  $\approx 0.5J$ , a surprisingly large value. In the spin-wave modelling, it was assumed that there is no magnetic contribution from the charge stripes; however, it is not obvious that this is a correct assumption. Combining an  $S = \frac{1}{2}$  hole with an  $S = 1$  Ni ion should leave at least an  $S = \frac{1}{2}$  per Ni site in a domain wall. Recently, Boothroyd *et al.* [167] have discovered quasi-1D magnetic scattering that disperses up to about 10 meV and becomes very weak above 100 K. This appears to correspond to the spin excitations of the charge stripes.

Inelastic neutron scattering measurements at  $T > T_{\text{co}}$  indicate that incommensurate spin fluctuations survive in the disordered state [168, 163], implying the existence of fluctuating stripes. This result is consistent with optical conductivity studies [169, 170] which show that while the dc conductivity approaches that of a metal above room temperature, the dynamic conductivity in the disordered state never shows the response of a conventional metal.

The overall message here is that a system very close to the cuprates shows a strong tendency for charge and spin to order in a manner that preserves the strong superexchange interaction of the undoped parent compound. It is certainly true that  $\text{Ni}^{2+}$  has  $S = 1$  while  $\text{Cu}^{2+}$  has  $S = \frac{1}{2}$ , and this can have a significant impact on the strength of the charge localization in the stripe-ordered nickelates [171]; however, the size of the spin cannot, on its own, explain why conventional band theory breaks down for the nickelates. The electronic inhomogeneity observed in the nickelates suggests that similarly unusual behavior might be expected in the cuprates.

### 8.5.2 Stripes in cuprates

Static charge and spin stripe orders have only been observed in a couple of cuprates,  $\text{La}_{1.875}\text{Ba}_{0.125}\text{CuO}_4$  [41] and  $\text{La}_{1.6-x}\text{Nd}_{0.4}\text{Sr}_x\text{CuO}_4$  [43, 172] to be specific. The characteristic 2D wave vector for spin order is  $\mathbf{q}_{\text{so}} = \mathbf{Q}_{\text{AF}} \pm (\epsilon, 0)$  and that for charge order is  $\mathbf{q}_{\text{co}} = (2\epsilon, 0)$ . A cartoon of stripe order consistent with these wave vectors is shown in Fig. 8.14(a); the inferred charge density within the charge stripes is approximately one hole for every two sites along the length of a stripe. The magnetic unit cell is twice as long as that for charge order. It should be noted that the phase of the stripe order with respect to the lattice has not been determined experimentally, so that it could be either bond-centered, as shown, or site-centered.

In a square lattice, the domains of vertical and horizontal stripes shown in Fig. 8.14 are equivalent; however, each breaks the rotational symmetry of the square lattice. In fact, static stripe order has only been observed in compounds in which the average crystal structure for each  $\text{CuO}_2$  plane exhibits a compatible reduction to rectangular symmetry. This is the case for the low-temperature-tetragonal (LTT) symmetry (space group  $P4_2/nm$ ) of  $\text{La}_{1.875}\text{Ba}_{0.125}\text{CuO}_4$  and  $\text{La}_{1.6-x}\text{Nd}_{0.4}\text{Sr}_x\text{CuO}_4$  [173], where orthogonal Cu-O bonds are inequivalent within each plane, but the special direction rotates



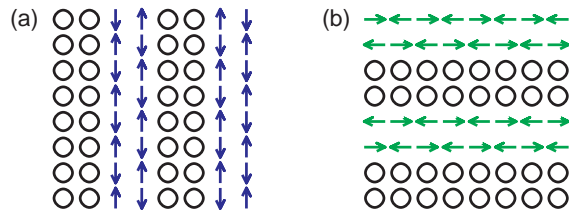


**Fig. 8.14.** Cartoons of equivalent domains of (a) vertical and (b) horizontal bond-centered stripe order within a  $\text{CuO}_2$  plane (only Cu sites shown). Note that the magnetic period is twice that of the charge period. The charge density along a stripe is one hole for every two sites in length.

by  $90^\circ$  from one layer to the next. Because planes of each orientation are equally represented in the LTT phase, both stripe domains are equally represented. The correlation between lattice symmetry and stripe ordering is especially clear in studies of the system  $\text{La}_{1.875}\text{Ba}_{0.125-x}\text{Sr}_x\text{CuO}_4$  by Fujita and coworkers [174, 175, 176].

When diffraction peaks from orthogonal stripe domains are present simultaneously, one might ask whether the diffraction pattern is also consistent with a checkerboard structure (a superposition of orthogonal stripe domains in the same layer) [177]. There are a number of arguments against a checkerboard interpretation. (1) The observed sensitivity of charge and spin ordering to lattice symmetry would have no obvious explanation for a checkerboard structure, with its 4-fold symmetry. (2) For a pattern of crossed stripes, the positions of the magnetic peaks should rotate by  $45^\circ$  with respect to the charge-order peaks. One would also expect to see additional charge-order peaks in the [110] direction. Tests for both of these possibilities have come out negative [178]. It is possible to imagine other two-dimensional patterns that are consistent with the observed diffraction peaks [177]; however, the physical justification for the relationship between the spin and charge modulation becomes unclear in such models. (3) The intensity of the charge-order scattering is strongly modulated along  $Q_z$ , with maxima at  $l = n \pm \frac{1}{2}$ , where  $n$  is an integer. This behavior is straightforwardly explained in terms of unidirectional stripe order tied to local lattice symmetry, with Coulomb repulsion between stripes in equivalent (next-nearest-neighbor) layers [179]. For a checkerboard pattern, one would expect correlations between nearest-neighbor layers, which would give a  $Q_z$  dependence inconsistent with experiment.

There has also been a report of stripe-like charge order and incommensurate spin fluctuations in a  $\text{YBa}_2\text{Cu}_3\text{O}_{6+x}$  sample with a nominal  $x = 0.35$  [180]. The superconducting transition for this sample, having a midpoint at 39 K and a width of 10 K, is a bit high to be consistent with the nominal oxygen content [143]; this may indicate some inhomogeneity of oxygen content in the very large melt-grown crystal that was studied. Weak superlattice peaks

attributed to charge order corresponding to vertical stripes with  $2\epsilon = 0.127$  retain finite intensity at room temperature. The difference in magnetic scattering at 10 K relative to 100 K shows a spectrum very similar to that in Fig. 8.3, with  $E_r \approx 23$  meV and  $\epsilon \approx 0.06$ . While these experimental results are quite intriguing, it would be desirable to confirm them on another sample. In any case, it is interesting to note that a recent muon spin rotation ( $\mu$ SR) study by Sanna *et al.* [181] identified local magnetic order at low temperatures in  $\text{YBa}_2\text{Cu}_3\text{O}_{6+x}$  with  $x \leq 0.39$ , and coexistence with superconductivity for  $x \geq 0.37$ .

Elastic incommensurate scattering consistent with stripe order has been observed in stage-4  $\text{La}_2\text{CuO}_{4+\delta}$  with  $T_c = 42$  K, although charge order has not been detected [55]. An interesting question is whether static stripe order coexists homogeneously with high-temperature superconductivity in this sample. The fact that the 4-layer staging of the oxygen interstitials creates two inequivalent types of  $\text{CuO}_2$  layers suggests the possibility that the order parameters for stripe order and superconductivity might have their maxima in different sets of layers. A  $\mu$ SR study of the same material found that only about 40% of the muons detected a local, static magnetic field [182]. While it was argued that the best fit to the time dependence of the zero-field muon spectra was obtained with an inhomogeneous island model, the data may also be compatible with a model of inhomogeneity perpendicular to the planes.

Beyond static order, we can consider the excitations of a stripe-ordered system. It has already been noted in §8.2.1 that the magnetic excitations of  $\text{La}_{1.875}\text{Ba}_{0.125}\text{CuO}_4$  at low temperature exhibit a similar dispersion to good superconductors without stripe order. The overall spectrum is only partially consistent with initial predictions of linear spin-wave theory for a stripe-ordered system [183, 184, 185]; however, it is reasonably reproduced by calculations that consider weakly-coupled two-leg spin ladders (of the type suggested by Fig. 8.14) [186, 187] or that treat both spin and electron-hole excitations of a stripe-ordered ground state [188].

The temperature dependence of the magnetic scattering at low energies ( $\leq 10$  meV) has been reported by Fujita *et al.* [41]; Fig. 8.15 shows some of the results. On the left, one can see that, in the stripe-ordered state ( $T = 8$  and 30 K), the  $\mathbf{Q}$ -integrated dynamic susceptibility is independent of frequency and temperature. Such behavior is consistent with expectations for spin waves. In the disordered phase (65 K and above),  $\tilde{\chi}''(\omega)$  heads linearly to zero at zero frequency; however, at 10 meV the decrease with temperature is relatively slow. The temperature dependence of  $\tilde{\chi}''(\omega)$  at 3 meV and 6 meV is shown in more detail on the right side, in panel (a). There is a rapid drop above  $T_{\text{co}}$  at 3 meV, but the change at 6 meV is more gradual. There is a substantial increase in  $\mathbf{Q}$  width of the incommensurate peaks at the transition, as shown in (b). Interestingly, there is also a significant drop in incommensurability at the transition, shown in (c), with a continuing decrease at higher temperatures. Similar results for  $\text{La}_{1.6-x}\text{Nd}_{0.4}\text{Sr}_x\text{CuO}_4$  with  $x = 0.12$  were obtained by

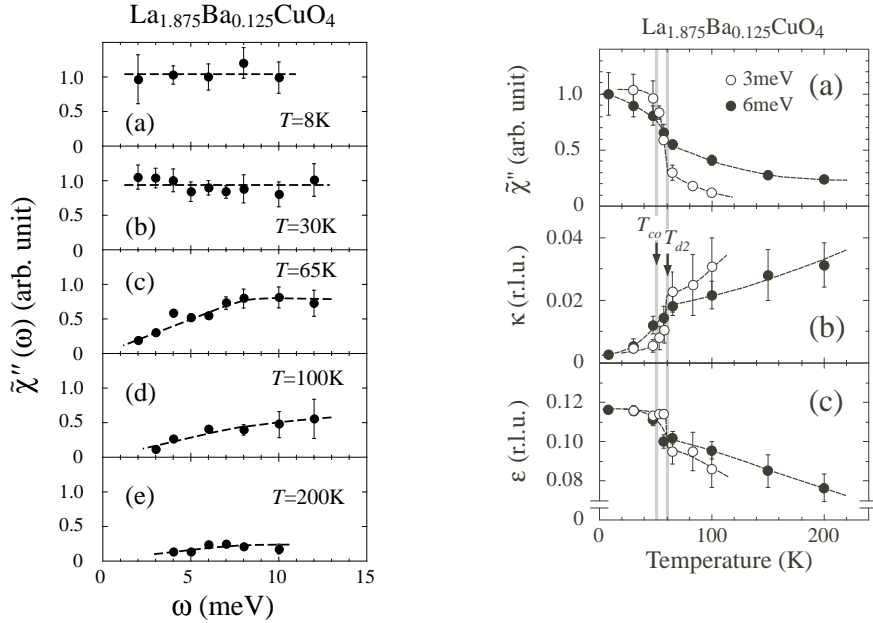


**Fig. 8.15.** Results for low-energy inelastic magnetic scattering in  $\text{La}_{1.875}\text{Ba}_{0.125}\text{CuO}_4$ . Left: local susceptibility,  $\tilde{\chi}''(\omega)$ , as a function of  $\hbar\omega$  for temperatures below [(a) and (b)] and above [(c)-(e)] the charge-ordering temperature,  $T_{\text{co}}$ . Right: Temperature dependence, for  $\hbar\omega = 3$  and 6 meV, of (a) local susceptibility, (b)  $\kappa$ , half-width in  $\mathbf{Q}$  of the incommensurate peaks, (c) incommensurability  $\epsilon$ . Vertical lines denote  $T_{\text{co}}$  and  $T_{d2}$ , the transition to the LTT phase. The dashed lines are guides to the eye. From Fujita *et al.* [41].

Ito *et al.* [189]. The jump in  $\epsilon$  on cooling through  $T_{\text{co}}$  may be related to commensurability effects in the stripe-ordered state.

The results in the disordered state ( $T > 60$  K) of  $\text{La}_{1.875}\text{Ba}_{0.125}\text{CuO}_4$  look similar to those found in the normal state of  $\text{La}_{2-x}\text{Sr}_x\text{CuO}_4$  [12]. The continuous variation of the magnetic scattering through the transition suggests that the nature of the underlying electronic correlations is the same on both sides of the transition. The simplest conclusion seems to be that dynamic stripes are present in the disordered state of  $\text{La}_{1.875}\text{Ba}_{0.125}\text{CuO}_4$  and in the normal state of  $\text{La}_{2-x}\text{Sr}_x\text{CuO}_4$ . The similarity of the magnetic spectrum to that in  $\text{YBa}_2\text{Cu}_3\text{O}_{6+x}$  (see Fig. 8.3) then suggests that dynamic stripes may be common to under- and optimally-doped cuprates.

### 8.5.3 Spin-density-wave order in chromium

Chromium and its alloys represent another system that has been proposed as a model for understanding the magnetic excitations in superconducting

cuprates [190]. Pure Cr has a body-centered-cubic structure and exhibits antiferromagnetic order that is slightly incommensurate [191]. Overhauser and Arrott [192] first proposed that the order was due to a spin-density-wave instability of the conduction electrons. Lomer [193] later showed that the amplitude of the SDW order could be understood in terms of approximate nesting of separate electron and hole Fermi surfaces. The ordering can be modified by adjusting the Fermi energy through small substitutions of neighboring 3d elements. For example, adding electrons through substitution of less than a percent of Mn is enough to drive the ordering wave vector to commensurability, whereas reducing the electron density with V causes the incommensurate ordering temperature to head to zero at a concentration of about 3.5% [190].

The magnetic excitations in pure Cr have a very large spin-wave velocity [194, 195], similar to the situation for cuprates. The results seem to be qualitatively consistent with calculations based on Fermi-surface nesting [196, 197]. A study of paramagnetic  $\text{Cr}_{0.95}\text{V}_{0.05}$  at low temperature [198] has revealed incommensurate excitations at low energy that broaden with increasing energy.  $\chi''$  has a peak at about 100 meV, but remains substantial up to at least 400 meV. A comparison of the magnitude of the experimental  $\chi''$  with *ab initio* calculations [199] indicates a substantial exchange enhancement over the bare Lindhard susceptibility [198].

Given that Cr is cubic, there are three equivalent and orthogonal nesting wave vectors. Within an ordered domain, the ordering wave vector consists of just one of these three possibilities. Along with the SDW order, there is also a weak CDW order that appears. A neutron diffraction study showed that the intensity of the CDW peaks scales as the square of the intensity of the SDW peaks, indicating that the CDW is a secondary order parameter and that the ordering transition is driven by the magnetic ordering [200]. It is natural to compare this behavior with that found in stripe ordered cuprates. The behavior in the latter is different, with the charge order peaks appearing at a higher temperature than those for spin order in  $\text{La}_{1.6-x}\text{Nd}_{0.4}\text{Sr}_x\text{CuO}_4$  with  $x = 0.12$  [201]. That result indicates that either charge ordering alone, or a combination of charge and spin energies, drive the initial ordering [202], so that stripe order is distinct from SDW order.

There are certainly some similarities between the magnetic excitations of Cr alloys and those of optimally-doped cuprates. The fact that the magnetism in Cr and its alloys is caused by Fermi-surface nesting has led many people to assume that a similar mechanism might explain the excitations of superconducting cuprates, as discussed elsewhere in this book. Some arguments against such an approach have been presented in Sec. VI of [203].

#### 8.5.4 Other proposed types of competing order

New types of order beyond spin-density waves or stripes have been proposed for cuprates. One is *d*-density-wave (DDW) order, which has been introduced by Chakravarty *et al.* [204] to explain the *d*-wave-like pseudogap seen by

photoemission experiments on underdoped cuprates. (A related model of a staggered-flux phase was proposed by Wen and Lee [205] with a similar motivation; however, their model does not have static order.) The model of DDW order involves local currents that rotate in opposite directions about neighboring plaquettes within the  $\text{CuO}_2$  planes. The orbital currents should induce weak, staggered magnetic moments oriented along the  $c$  axis. Because of the large size of the current path in real space, the magnetic form factor should fall off very rapidly with  $\mathbf{Q}_{2D}$  in reciprocal space. Mook *et al.* [206] have done extensive measurements in search of the proposed signal in  $\text{YBa}_2\text{Cu}_3\text{O}_{6+x}$  with several values of  $x$ . The measurements are complicated by the fact that large crystals are required to achieve the necessary sensitivity, while the largest crystals available are contaminated by a significant amount of  $\text{Y}_2\text{BaCuO}_5$ . Stock *et al.* [207] studied a crystal of  $\text{YBa}_2\text{Cu}_3\text{O}_{6.5}$  with unpolarized neutrons, and concluded that no ordered moment could be seen to a sensitivity of  $\sim 0.003 \mu_B$ . Using polarized neutrons, Mook *et al.* [208] have seen, in the spin-flip channel, a weak peak at  $\mathbf{Q}_{AF}$  on top of a large background. Without giving an error bar, they suggest that the associated moment might be  $0.0025 \mu_B$ . They concluded that “the present results provide indications that orbital current phases are not ruled out” [208].

Varma [209] has proposed a different model of ordered orbital currents, in which the currents flow between a single Cu ion and its four coplanar O neighbors. This state breaks time-reversal and rotational symmetry but not translational symmetry. Thus, magnetic scattering from the  $c$ -axis-oriented orbital moments should be superimposed on nuclear Bragg scattering from the crystal lattice. Information on the nature of the orbital currents is contained in a strongly  $\mathbf{Q}$ -dependent structure factor. The only practical way to detect such a small magnetic signal on top of the strong nuclear peaks would be with polarized neutrons. Lee *et al.* [210] performed extensive polarized-beam studies on  $\text{La}_{2-x}\text{Sr}_x\text{CuO}_4$  and  $\text{YBa}_2\text{Cu}_3\text{O}_{6+x}$  single crystals. They found no positive evidence for the proposed magnetic moments, with a sensitivity of  $0.01 \mu_B$  in the case of 3D order, and  $0.1 \mu_B$  in the case of quasi-2D order. Simon and Varma [211] have since proposed a second pattern of orbital currents that would have a different magnetic structure factor from the original version. Positive results in  $\text{YBa}_2\text{Cu}_3\text{O}_{6+x}$  corresponding to this second pattern have recently been reported by Fauqué *et al.* [212].

## 8.6 Variation of magnetic correlations with doping and temperature in cuprates

### 8.6.1 Magnetic incommensurability vs. hole doping

The doping dependence of the low-energy magnetic excitations in superconducting  $\text{La}_{2-x}\text{Sr}_x\text{CuO}_4$  have been studied in considerable detail [13, 131]. In particular, the  $\mathbf{Q}$  dependence has been characterized. We already saw in §8.4

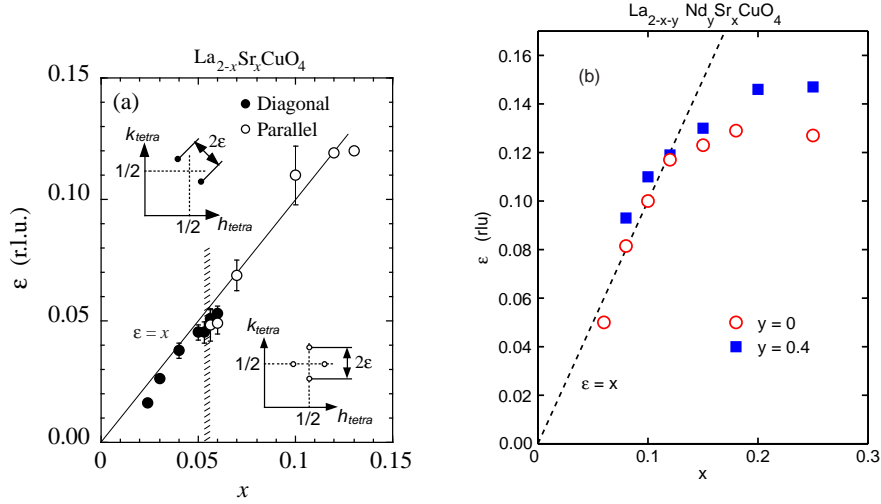


**Fig. 8.16.** Variation of the magnetic incommensurability  $\epsilon$  [as defined in the insets of (a)] for (a) lightly-doped  $\text{La}_{2-x}\text{Sr}_x\text{CuO}_4$ , and (b)  $\text{La}_{2-x}\text{Sr}_x\text{CuO}_4$  with and without Nd-codoping. In (a) the filled (open) symbols correspond to diagonal (bond-parallel, or vertical) spin stripes. Adapted from Fujita *et al.* [131]. In (b), open circles are from measurements of excitations at  $E \sim 3$  meV and  $T \approx T_c$  in  $\text{La}_{2-x}\text{Sr}_x\text{CuO}_4$  from Yamada *et al.* [13]; filled squares are from elastic scattering on  $\text{La}_{1.6-x}\text{Nd}_{0.4}\text{Sr}_x\text{CuO}_4$  from Ichikawa *et al.* [172].

that the destruction of antiferromagnetic order by hole doping leads to diagonal spin stripes. As shown in Fig. 8.16(a), the magnetic incommensurability  $\epsilon$  grows roughly linearly with  $x$  across the “spin-glass” regime. (The results in this region are from elastic scattering.) At  $x \approx 0.055$ , there is an insulator to superconductor transition, and along with that is a rotation of the incommensurate peaks (as shown in the insets), indicating a shift from diagonal to vertical (or bond-parallel) stripes [131]. The rotation of the stripes is not as sharply defined as is the onset of the superconductivity—there is a more gradual evolution of the distribution of stripe orientations as indicated by the measured peak widths, especially around the circle of radius  $\epsilon$  centered on  $\mathbf{Q}_{\text{AF}}$ . Interestingly, the magnitude of  $\epsilon$  continues its linear  $x$  dependence through the onset of superconductivity.

In the superconducting phase,  $\epsilon$  continues to grow with doping up to  $x \sim \frac{1}{8}$ , beyond which it seems to saturate, as indicated by the circles [13] in Fig. 8.16(b). Interestingly, the same trend in incommensurability is found for static stripe order in Nd-doped  $\text{La}_{2-x}\text{Sr}_x\text{CuO}_4$  [172], as indicated by the filled squares in the same figure. The differences in wave vector for a given  $x$  may reflect a change in the hole density of the charge stripes when they become statically ordered in the anisotropic lattice potential of the LTT phase.

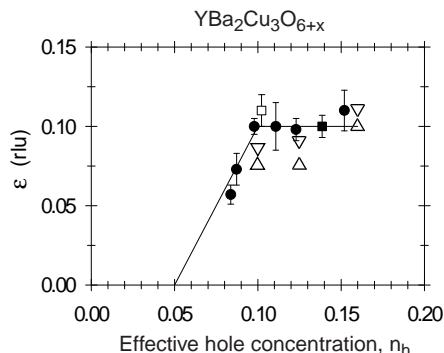


**Fig. 8.17.** Magnetic incommensurability in  $\text{YBa}_2\text{Cu}_3\text{O}_{6+x}$  (circles and squares) measured just above the spin-gap energy at  $T \ll T_c$ , with  $n_h$  estimated from  $T_c$ , from Dai *et al.* [17]. The triangles indicate the incommensurability at 20 meV (upper) and 30 meV (lower) for  $\text{La}_{2-x}\text{Sr}_x\text{CuO}_4$  with  $x = 0.10$  and  $0.16$  [40] and  $\text{La}_{1.875}\text{Ba}_{0.125}\text{CuO}_4$  [42].

While low-energy incommensurate scattering is also observed in overdoped  $\text{La}_{2-x}\text{Sr}_x\text{CuO}_4$ , Wakimoto *et al.* [213] have found that the magnitude of  $\chi''$ , measured at  $E \sim 6$  meV, drops rapidly for  $x > 0.25$ , becoming negligible by  $x = 0.30$ . The decrease in the magnitude of  $\chi''$  is correlated with the fall off in  $T_c$ . Interestingly, these results suggest that the superconductivity weakens as magnetic correlations disappear.

In  $\text{YBa}_2\text{Cu}_3\text{O}_{6+x}$ , the incommensurability of the magnetic excitations at  $E < E_r$  is resolvable only for  $T \ll T_c$ . The presence of a substantial spin gap in the superconducting state, together with the dispersion of the magnetic excitations, makes it difficult to compare directly the results for  $\text{YBa}_2\text{Cu}_3\text{O}_{6+x}$  with the behavior of  $\text{La}_{2-x}\text{Sr}_x\text{CuO}_4$  shown in Fig. 8.16(b). Dai *et al.* [17] have determined  $\epsilon$  at energies just above the spin gap; the results for  $\text{YBa}_2\text{Cu}_3\text{O}_{6+x}$  are represented by circles and squares in Fig. 8.17. For comparison, the triangles indicate the effective incommensurabilities found at energies of 20 and 30 meV in  $\text{La}_{2-x}\text{Sr}_x\text{CuO}_4$  with  $x = 0.10$  and  $0.16$  [40] and in  $\text{La}_{1.875}\text{Ba}_{0.125}\text{CuO}_4$  [42]. The trends in the two different cuprate families seem to be similar when one accounts for the dispersion. (Comparable behavior in  $\text{YBa}_2\text{Cu}_3\text{O}_{6+x}$  and  $\text{La}_{2-x}\text{Sr}_x\text{CuO}_4$  was also noted by Balatsky and Bourges [214].)

### 8.6.2 Doping dependence of energy scales

The doping dependence of  $E_r$  in  $\text{YBa}_2\text{Cu}_3\text{O}_{6+x}$  and  $\text{Bi}_2\text{Sr}_2\text{CaCu}_2\text{O}_{8+\delta}$  has received considerable attention. In optimally-doped and slightly under-doped  $\text{YBa}_2\text{Cu}_3\text{O}_{6+x}$ , the scattering at  $E_r$  (for  $T < T_c$ ) is relatively strong and narrow in  $\mathbf{Q}$  and  $\omega$ . Of course, when the intensity is integrated over  $\mathbf{Q}$  and  $\omega$  one finds that it corresponds to a small fraction of the total expected sum-rule

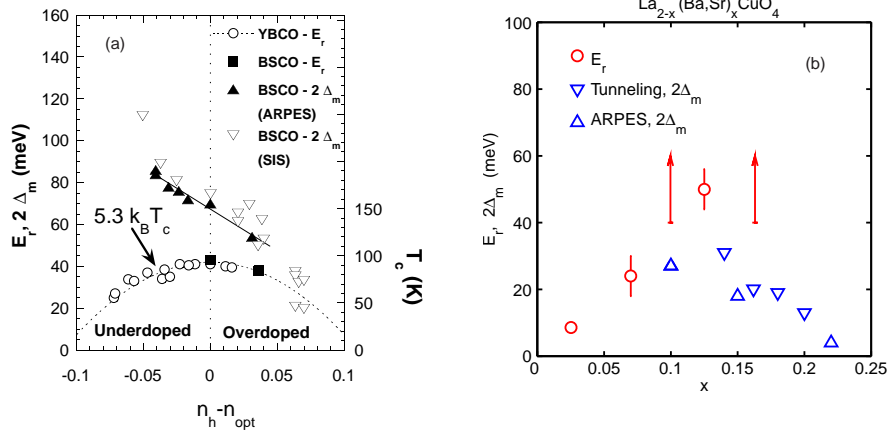


**Fig. 8.18.** (a) Summary of results for the resonance energy  $E_r$  from neutron scattering measurements on  $YBa_2Cu_3O_{6+x}$  (open circles) and  $Bi_2Sr_2CaCu_2O_{8+\delta}$  (filled squares), and twice the maximum of the superconducting gap,  $2\Delta_m$ , from angle-resolved photoemission (ARPES, filled triangles) and tunneling (open triangles) measurements on  $Bi_2Sr_2CaCu_2O_{8+\delta}$ , taken from Sidis *et al.* [18]. (b)  $E_r$  (circles) for  $La_{1.875}Ba_{0.125}CuO_4$  [42] and estimated for  $La_{2-x}Sr_xCuO_4$  from measurements on  $x = 0.024$  [129],  $x = 0.07$  [215],  $x = 0.10$  and  $0.16$  [40];  $2\Delta_m$  for  $La_{2-x}Sr_xCuO_4$  from tunneling (downward triangles) [216, 217] and ARPES (upward triangles) [218].

weight [26]; it is also a small fraction of the the total spectral weight that is actually measured (which is much reduced from that predicted by the sum rule [90]).

Figure 8.18(a) presents a summary, from Sidis *et al.* [18], of experimental results for  $E_r$  from neutron scattering and for twice the superconducting gap maximum,  $2\Delta_m$ , from other techniques. For these materials, the resonance energy is found to scale with  $T_c$  and fall below  $2\Delta_m$ . Unfortunately, a major deviation from these trends occurs in  $La_{2-x}Sr_xCuO_4$  [see Fig. 8.18(b)], where  $E_r$  tends to be larger than  $2\Delta_m$ , and any constant of proportionality between  $E_r$  and  $kT_c$  is considerably larger than the value of  $\sim 5$  found for  $YBa_2Cu_3O_{6+x}$ .

As discussed in §8.2.2, there may be a more general correlation between the spin-gap energy and  $T_c$ . Figure 8.19 shows the variation of the spin-gap energy with  $T_c$  for a range of dopings in  $YBa_2Cu_3O_{6+x}$  as obtained by Dai *et al.* [17]. The correlation seen there looks very much like that shown in Fig. 8.6 for different cuprate families at optimum doping. For  $La_{2-x}Sr_xCuO_4$ , a true spin gap is not observed for  $x < 0.14$  [219], and this might have a connection with the rapid disappearance of the spin gap in  $YBa_2Cu_3O_{6+x}$  for  $x < 0.5$  [17].



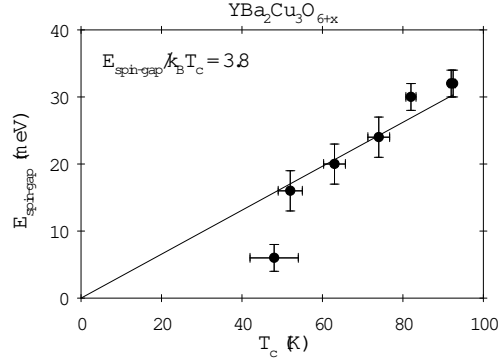


**Fig. 8.19.** Spin-gap energy vs.  $T_c$  for  $\text{YBa}_2\text{Cu}_3\text{O}_{6+x}$  from Dai *et al.* [17].

### 8.6.3 Temperature-dependent effects

A detailed study of the thermal evolution of the magnetic excitations ( $E \leq 15$  meV) in  $\text{La}_{1.86}\text{Sr}_{0.14}\text{CuO}_4$  was reported by Aeppli *et al.* [12]. Fitting the  $\mathbf{Q}$  dependence of the incommensurate scattering with a lorentzian-squared peak shape, they found that  $\kappa$ , the  $Q$ -width as a function of both frequency and temperature, can be described fairly well by the formula

$$\kappa^2 = \kappa_0^2 + \frac{1}{a^2} \left[ \left( \frac{kT}{E_0} \right)^2 + \left( \frac{\hbar\omega}{E_0} \right)^2 \right], \quad (8.12)$$

where  $\kappa_0 = 0.034 \text{ \AA}^{-1}$ ,  $a$  is the lattice parameter, and  $E_0 = 47$  meV. For  $T \geq T_c$ , the low-frequency limit of  $\chi''(\mathbf{Q}_\delta, \omega)/\omega$  (where  $\mathbf{Q}_\delta$  is a peak position) varies with temperature essentially as  $1/T^2$ . They argued that these behaviors are consistent with proximity to a quantum critical point, and that the type of ordered state that is being approached at low temperature is the stripe-ordered state.

In a study of  $\text{La}_{2-x}\text{Sr}_x\text{CuO}_4$  crystals at somewhat higher doping ( $x = 0.15, 0.18, \text{ and } 0.20$ ), Lee *et al.* [220] found evidence for a spin pseudogap at  $T \geq T_c$ . The pseudogap (with a hump above it) was similar in energy to the spin gap that appears at  $T < T_c$  and was most distinct in the  $x = 0.18$  sample, where the effect is still evident at 80 K but absent at 150 K.

For  $\text{YBa}_2\text{Cu}_3\text{O}_{6+x}$ , the studies of temperature dependence have largely concentrated on the scattering near  $E_r$ . For fully-oxygenated  $\text{YBa}_2\text{Cu}_3\text{O}_7$ , the intensity at  $E_r$  appears fairly abruptly at, or slightly below,  $T_c$  and grows with decreasing temperature, with essentially no shift in  $E_r$  [16, 31]. For underdoped samples, the intensity at  $E_r$  begins to grow below temperatures  $T^* > T_c$ , with the enhancement at  $T_c$  decreasing with underdoping [31, 36, 47].

## 8.7 Effects of perturbations on magnetic correlations

### 8.7.1 Magnetic field

An important initial study of the impact of an applied magnetic field on magnetic correlations in a cuprate superconductor was done by Dai *et al.* [50] on  $\text{YBa}_2\text{Cu}_3\text{O}_{6.6}$  ( $T_c = 63$  K). They showed that applying a 6.8-T field along the  $c$ -axis caused a 30% reduction in the low-temperature intensity of the resonance peak (at 34 meV). The lost weight presumably is shifted to other parts of phase space, but it was not directly detected. (Applying the field parallel to the  $\text{CuO}_2$  planes has negligible effect.) In an earlier study on  $\text{YBa}_2\text{Cu}_3\text{O}_7$ , Bourges *et al.* [221] applied an 11.5 T field and found that the resonance peak broadened in energy but did not seem to change its peak intensity. The difference in response from  $\text{YBa}_2\text{Cu}_3\text{O}_{6.6}$  is likely due to the difference in  $H_{c2}$ , which is about 5 times larger in  $\text{YBa}_2\text{Cu}_3\text{O}_7$  [222].

A series of studies on  $\text{La}_{2-x}\text{Sr}_x\text{CuO}_4$  samples with various dopings have now been performed [223, 52, 224, 51, 223], and a schematic summary of the results is presented in Fig. 8.20. For samples with lower doping ( $x = 0.10$  [224] and  $0.12$  [223]) there is a small elastic, incommensurate, magnetic peak intensity in zero field that is substantially enhanced by application of a  $c$ -axis magnetic field. The growth of the intensity with field is consistent with

$$I \sim (H/H_{c2}) \ln(H_{c2}/H), \quad (8.13)$$

where  $H_{c2}$  is the upper critical field for superconductivity [224]. This behavior was predicted by Demler *et al.* [225] using a model of coexisting but competing phases of superconductivity and spin-density-wave (SDW) order. In their model, local reduction of the superconducting order parameter by magnetic vortices results in an average increase in the SDW order. (For an alternative approach, in which the competing order is restricted to “halo” regions centered on vortex cores, see, e.g., [226].) Interestingly, the spin-spin correlation length for the induced signal is  $> 400$  Å, which is at least 20 times greater than the radius of a vortex core [224]. Very similar results have been obtained on oxygen-doped  $\text{La}_2\text{CuO}_4$  [227, 228]. There is an obvious parallel with the charge-related “checkerboard” pattern observed at vortices in superconducting  $\text{Bi}_2\text{Sr}_2\text{CaCu}_2\text{O}_{8+\delta}$  by scanning tunneling microscopy [229].

For  $\text{La}_{2-x}\text{Sr}_x\text{CuO}_4$  crystals with  $x = 0.163$  [52] and  $0.18$  [51] there is no field-induced static order (at least for the range of fields studied). Instead, the field moves spectral weight into the spin gap. The study on  $x = 0.18$  indicated that the increase in weight in the gap is accompanied by a decrease in the intensity peak above the gap [51], the latter result being comparable to the effect seen in  $\text{YBa}_2\text{Cu}_3\text{O}_{6.6}$  [50]. For  $x = 0.163$ , an enhancement of the incommensurate scattering was observed below 10 K for  $\hbar\omega = 2.5$  meV.

For an intermediate doping concentration of  $x = 0.144$ , Khaykovich *et al.* [230] have recently shown that, although no elastic magnetic peaks are seen at zero field, a static SDW does appear for  $H > H_c \sim 3$  T. Such behavior

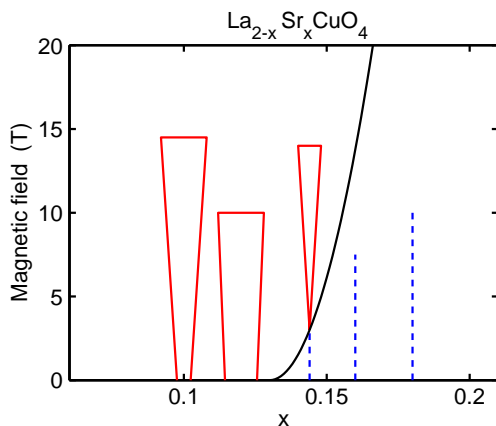


**Fig. 8.20.** Schematic summary of neutron scattering experiments on  $\text{La}_{2-x}\text{Sr}_x\text{CuO}_4$  in a magnetic field at  $T \ll T_c$ . Solid bars indicate observations of elastic, incommensurate peaks; width indicates variation of peak intensity with field. Experiments on  $x = 0.10, 0.12, 0.144, 0.163,$  and  $0.18$  from [224],[223], [230], [52], and [51]. The solid curve suggests the shape of a boundary between a state with spin-density-wave order and superconductivity on the left and superconductivity alone on the right, as first proposed by Demler *et al.* [225].

was predicted by the model of competing phases of Demler *et al.* [225], and a boundary between phases with and without SDW order, based on that model, is indicated by the solid curve in Fig. 8.20.

Although evidence for field-induced charge-stripe order in  $\text{La}_{2-x}\text{Sr}_x\text{CuO}_4$  has not yet been reported, it seems likely that the SDW order observed is the same as the stripe phase found in  $\text{La}_{1.875}\text{Ba}_{0.125}\text{CuO}_4$  [41] and  $\text{La}_{1.6-x}\text{Nd}_{0.4}\text{Sr}_x\text{CuO}_4$  [172]. Consistent with this scenario, it has been shown that an applied magnetic field has no impact on the Cu magnetic order or the charge order in the stripe-ordered phase of  $\text{La}_{1.6-x}\text{Nd}_{0.4}\text{Sr}_x\text{CuO}_4$  with  $x = 0.15$  [231]; however, the field did effect the ordering of the Nd “spectator” moments.

Returning to  $\text{La}_{2-x}\text{Sr}_x\text{CuO}_4$  with  $x < 0.13$ , it has been argued in the case of  $x = 0.10$  that the zero-field elastic magnetic peak intensity observed at low temperature is extrinsic [224]. This issue deserves a short digression. It is certainly true that crystals of lesser quality can yield elastic scattering at or near the expected positions of the incommensurate magnetic peaks; in some cases, this scattering has little temperature dependence. Of course, just because spurious signals can occur does not mean that all signals are spurious. Let us shift our attention for a moment to  $x = 0.12$ , where the low-temperature, zero-field intensity is somewhat larger [232]. A muon-spin-relaxation ( $\mu\text{SR}$ ) study [182] on a crystal of good quality has shown that the magnetic order is not uniform in the sample—at low temperature, only  $\sim 20\%$

of the muons see a static local hyperfine field. Further relevant information comes from electron diffraction studies. The well-known low-temperature orthorhombic (LTO) phase tends to exhibit twin domains. Horibe, Inoue, and Koyama [233] have taken dark-field images using a Bragg peak forbidden in the LTO structure but allowed in the LTT structure, the phase that pins stripes in  $\text{La}_{1.875}\text{Ba}_{0.125}\text{CuO}_4$  and  $\text{La}_{1.6-x}\text{Nd}_{0.4}\text{Sr}_x\text{CuO}_4$ . They find bright lines corresponding to the twin boundaries, indicating that the structure of the twin boundaries is different from the LTO phase but similar to the LTT. (Similar behavior has been studied in  $\text{La}_{2-x}\text{Ba}_x\text{CuO}_4$  [234].) The twin boundaries are only a few nanometers wide; however, given that magnetic vortices can pin spin stripes with a substantial correlation length, and we will see next that Zn dopants can also pin spin stripes, it seems likely that LTT-like twin boundaries should be able to pin stripe order with a significant correlation length. Thus, the low-temperature magnetic peaks found in  $\text{La}_{2-x}\text{Sr}_x\text{CuO}_4$  with  $x = 0.12$  [232] are likely due to stripes pinned at twinned boundaries, giving order in only a small volume fraction, consistent with  $\mu\text{SR}$  [182]. Taking into account the fact that stripe order is observed in  $\text{La}_{1.6-x}\text{Nd}_{0.4}\text{Sr}_x\text{CuO}_4$  for a substantial range of  $x$  (but with strongest ordering at  $x = 0.12$ ) [172], it seems reasonable to expect a small volume fraction of stripe order pinned at twin boundaries in  $\text{La}_{2-x}\text{Sr}_x\text{CuO}_4$  with  $x = 0.10$ . Is this order extrinsic? Are twin boundaries extrinsic? This may be a matter of semantics. In any case, I would argue that the low-temperature zero-field peaks measured in good crystals reflect real materials physics of the pure compound.

### 8.7.2 Zn substitution

The effects of Zn substitution for Cu are quite similar to those caused by an applied magnetic field. For  $\text{La}_{2-x}\text{Sr}_x\text{CuO}_4$  with  $x = 0.15$ , substituting about 1% or less Zn causes the appearance of excitations within the spin gap of the Zn-free compound [235, 236]. Substitution of 1.7% Zn is sufficient to induce weak elastic magnetic peaks. For  $x = 0.12$ , where weak elastic magnetic peaks are present without Zn, substitution of Zn increases the peak intensity, but also increases the  $Q$ -widths of the peaks [237, 178]. Wakimoto *et al.* [238] have recently found that Zn-substitution into overdoped samples ( $x > 0.2$ ) significantly enhances the low-energy ( $< 10$  meV) inelastic magnetic scattering.

In  $\text{YBa}_2\text{Cu}_3\text{O}_{6+x}$ , Zn substitution causes weight to shift from  $E_r$  into the spin gap [239, 240]. While it causes some increase in the  $Q$ -width of the scattering at  $E_r$  [241], it does not make a significant change in the  $\mathbf{Q}$  dependence of the (unresolved) incommensurate scattering at lower energies [240]. Muon-spin rotation studies indicate that Zn-doping reduces the superfluid density proportional to the Zn concentration [242], and this provides another parallel with the properties of the magnetic vortex state.

### 8.7.3 Li-doping

An alternative way to dope holes into the  $\text{CuO}_2$  planes is to substitute  $\text{Li}^{1+}$  for  $\text{Cu}^{2+}$ . In this case, the holes are introduced at the expense of a strong local Coulomb potential that one might expect to localize the holes. Surprisingly, the magnetic phase diagram of  $\text{La}_2\text{Cu}_{1-x}\text{Li}_x\text{O}_4$  is rather similar to that for  $\text{La}_{2-x}\text{Sr}_x\text{CuO}_4$  with  $x < 0.06$  [243]. In particular, the long-range Néel order is destroyed with  $\sim 0.03\%$  Li. The nature of the magnetic correlations in the paramagnetic phase is different from that in  $\text{La}_{2-x}\text{Sr}_x\text{CuO}_4$  in that the inelastic magnetic scattering remains commensurate [244]. Studies of the spin dynamics indicate  $\omega/T$  scaling at high temperatures, but large deviations from such behavior occur at low temperature [245].

## 8.8 Electron-doped cuprates

Electron-doped cuprates are very interesting because of their similarities and differences from the hole-doped materials; however, considerably less has been done in the way of neutron scattering on the electron-doped materials, due in part to challenges in growing crystals of suitable size and quality. Initial work focused on the systems  $\text{Nd}_{2-x}\text{Ce}_x\text{CuO}_4$  and  $\text{Pr}_{2-x}\text{Ce}_x\text{CuO}_4$ . A striking difference from hole doping is the fact that the Néel temperature is only gradually reduced by electron-doping. This was first demonstrated in a  $\mu\text{SR}$  study of  $\text{Nd}_{2-x}\text{Ce}_x\text{CuO}_4$  [246], where it was found that the antiferromagnetic order only disappears at  $x \approx 0.14$  where superconductivity first appears. The magnetic order was soon confirmed by neutron diffraction measurements on single crystals of  $\text{Pr}_{2-x}\text{Ce}_x\text{CuO}_4$  [247] and  $\text{Nd}_{2-x}\text{Ce}_x\text{CuO}_4$  [248].

A complication with these materials is that to obtain the superconducting phase, one must remove a small amount of oxygen from the as-grown samples. The challenge of the reduction process is to obtain a uniform oxygen concentration in the final sample. This is more easily done in powders and thin films than in large crystals. As grown crystals with  $x$  as large as 0.18 are antiferromagnetic [249, 250]. Reducing single crystals can result in superconductivity; however, it is challenging to completely eliminate the antiferromagnetic phase [249]. In trying to get a pure superconducting phase, the reducing conditions can sometimes cause a crystal to undergo partial decomposition, yielding impurity phases such as  $(\text{Nd,Ce})_2\text{O}_3$  [251, 252].

The effective strength of the spin-spin coupling has been probed through measurements of the spin correlation length as a function of temperature in the paramagnetic phase. The magnitude of the spin stiffness is clearly observed to decrease with doping [247, 249, 250]. Mang *et al.* [250] have shown that this behavior is consistent with that found in numerical simulations of a randomly site-diluted 2D antiferromagnet. In the model calculations, the superexchange energy is held constant, and the reduction in spin stiffness is due purely to the introduction of a finite concentration of nonmagnetic sites. To get quantitative

agreement, it is necessary to allow for the concentration of nonmagnetic sites in the model to be about 20% greater than the Ce concentration in the samples.

Yamada and coworkers [253] were able to prepare crystals of  $\text{Nd}_{1.85}\text{Ce}_{0.15}\text{CuO}_4$  with sufficient quality that it was possible to study the low-energy magnetic excitations associated with the superconducting phase. They found commensurate antiferromagnetic fluctuations. In a crystal with  $T_c = 25$  K, they found that a spin gap of approximately 4 meV developed in the superconducting state. Commensurate elastic scattering, with an in-plane correlation length of 150 Å, was also present for temperatures below  $\sim 60$  K; however, the growth of the elastic intensity did not change on crossing the superconducting  $T_c$ .

While the magnetic excitations are commensurate and incompatible with stripe correlations, there are, nevertheless, other measurements that suggest electronic inhomogeneity. Henggeler *et al.* [254] used the crystal-field excitations of the Pr ions in  $\text{Pr}_{2-x}\text{Ce}_x\text{CuO}_4$  as a probe of the local environment. They found evidence for several distinct local environments, and argued that doped regions reached the percolation limit at  $x \approx 0.14$ , at the phase boundary for superconductivity. Recent NMR studies have also found evidence of electronic inhomogeneity [255, 256].

Motivated by the observation of magnetic-field-induced magnetic superlattice peaks in hole-doped cuprates (§8.7.1), there has been a series of experiments looking at the effect on electron-doped cuprates of a field applied along the  $c$  axis. An initial study [257] on  $\text{Nd}_{2-x}\text{Ce}_x\text{CuO}_4$  with  $x = 0.14$  and  $T_c \sim 25$  K found that applying a field as large as 10 T had no effect on the intensity of an antiferromagnetic Bragg peak for temperatures down to 15 K. Shortly after that came a report [258] of large field-induced enhancements of antiferromagnetic Bragg intensities, as well as new field-induced peaks of the type  $(\frac{1}{2}, 0, 0)$ , in a crystal of  $\text{Nd}_{2-x}\text{Ce}_x\text{CuO}_4$  with  $x = 0.15$  and  $T_c = 25$  K. It was soon pointed out that the new  $(\frac{1}{2}, 0, 0)$  peaks, as well as most of the effects at antiferromagnetic reflections, could be explained by the magnetic response of the  $(\text{Nd,Ce})_2\text{O}_3$  impurity phase [251, 252]. There now seems to be a consensus that this is the proper explanation [259, 260]; however, a modest field-induced intensity enhancement has been seen at  $(\frac{1}{2}, \frac{1}{2}, 3)$  that is not explained by the impurity-phase model [259].

In an attempt to clarify the situation, Fujita *et al.* [261] turned to another electron-doped superconductor,  $\text{Pr}_{1-x}\text{LaCe}_x\text{CuO}_4$ . This compound also has to be reduced to obtain superconductivity, and reduced crystals exhibit a  $(\text{Pr,Ce})_2\text{O}_3$  impurity phase; however, the Pr in the impurity phase should not be magnetic. They found a weak field-induced enhancement of an antiferromagnetic peak intensity for a crystal with  $x = 0.11$  ( $T_c = 26$  K), but no effect for  $x = 0.15$  ( $T_c = 16$  K). The induced Cu moment for  $x = 0.11$  at a temperature of 3 K and a field of 5 T is  $\sim 10^{-4} \mu_B$ . Dai and coworkers [262, 263] have studied crystals of  $\text{Pr}_{0.88}\text{LaCe}_{0.12}\text{CuO}_{4-\delta}$  in which they have tuned the superconductivity by adjusting  $\delta$ . They have emphasized the coexistence of the superconductivity with both 3D and quasi-2D antiferro-

magnetic order [262]. They report a very slight enhancement of the quasi-2D antiferromagnetic signal for a  $c$ -axis magnetic field [263].

## 8.9 Discussion

### 8.9.1 Summary of experimental trends in hole-doped cuprates

There are a number of trends in hole-doped cuprates that one can identify from the results presented in this chapter. To begin with, the undoped parent compounds are Mott-Hubbard (or, more properly, charge-transfer) insulators that exhibit Néel order due to antiferromagnetic superexchange interactions between nearest-neighbor atoms. The magnitude of  $J$  is material dependent, varying between roughly 100 and 150 meV.

Doping the  $\text{CuO}_2$  planes with holes destroys the Néel order; in fact, the presence of holes seems to be incompatible with long-range antiferromagnetic order. The observed responses to hole doping indicate that some sort of phase separation is common. In some cases, stripe modulations are found, and in others, finite clusters of antiferromagnetic order survive.

In under- and optimally-doped cuprate superconductors, the magnetic spectrum has an hour-glass-like shape, with an energy scale comparable to the superexchange energy of the parent insulators. The strength of the magnetic scattering, when integrated over momentum and energy, decreases gradually as one increases the hole concentration from zero to optimal doping. A spin gap appears in the superconducting state (at least for optimal doping), with spectral weight from below the spin gap being pushed above it. The magnitude of the spin gap correlates with  $T_c$ .

Underdoped cuprates with a small or negligible spin gap are very sensitive to perturbations. Substituting non-magnetic Zn for Cu or applying a magnetic field perpendicular to the planes tends to induce elastic incommensurate magnetic peaks at low temperature. For samples with larger spin gaps, the perturbations shift spectral weight from higher energy into the spin gap. Breaking the equivalence between orthogonal Cu-O bonds within a  $\text{CuO}_2$  plane can result in charge-stripe order, in addition to the elastic magnetic peaks.

The magnetic correlations within the  $\text{CuO}_2$  planes are clearly quite sensitive to hole doping and superconductivity. While their coexistence with a metallic normal state is one of the striking characteristics of the cuprates, their connection to the mechanism of hole-pairing remains a matter of theoretical speculation.

### 8.9.2 Theoretical interpretations

The nature and relevance of antiferromagnetic correlations has been a major theme of much of the theoretical work on cuprate superconductors. While

some the theoretical concepts are discussed in more detail in other chapters of this book, it seems appropriate to briefly review some of them here.

Given that techniques for handling strongly-correlated hole-doped antiferromagnets continue to be in the development stage, some researchers choose to rely on a conventional weak-coupling approach to describing magnetic metals. This might be appropriate if one imagines starting out in the very over-doped regime, where Fermi-liquid theory might be applicable, and then works downward towards optimum doping. The magnetic susceptibility can be calculated in terms of electrons being excited across the Fermi level from filled to empty states. Interactions between quasiparticles due to Coulomb or exchange interactions are assumed to enhance the susceptibility near  $\mathbf{Q}_{\text{AF}}$ , and this is handled using the random-phase approximation (RPA). In the superconducting state, one takes into account the superconducting gap  $\Delta$  with  $d$ -wave symmetry. The gapping of states carves holes into the continuum of electron-hole excitations. The RPA enhancement can then pull resonant excitations down into the region below  $2\Delta$  [264, 265, 266]. With this approach, it has been possible, with suitable adjustment of the interaction parameter, to calculate dispersing features in  $\chi''$  that resemble those measured in the superconducting state of optimally-doped  $\text{YBa}_2\text{Cu}_3\text{O}_{6+x}$  [267, 268, 269].

The RPA approach runs into difficulties when one considers  $\text{La}_{2-x}\text{Sr}_x\text{CuO}_4$ ,  $\text{La}_{2-x}\text{Ba}_x\text{CuO}_4$ , and underdoped  $\text{YBa}_2\text{Cu}_3\text{O}_{6+x}$ . It predicts that the magnetic excitations should be highly over damped at energies greater than  $2\Delta$ ; however, there is no obvious change in the experimental spectra at  $E > 2\Delta$  in these materials. Furthermore, the dispersive features in  $\text{La}_{1.875}\text{Ba}_{0.125}\text{CuO}_4$  are observed in the normal state. Even if one tries to invoke a  $d$ -wave pseudogap, the energy scale is likely to be too small, as indicated by Fig. 8.18(b). It is also unclear how one would rationalize, from a Fermi-liquid perspective, the observation that the energy scale of the magnetic excitations is of order  $J$ , as superexchange is an effective interaction between local moments in a correlated insulator, and has no direct connection to interactions between quasiparticles [53].

The fact that superexchange seems to remain relevant in the superconducting phase suggests that it may be profitable to approach the problem from the perspective of doped antiferromagnets. The resonating-valence-bond model was one of the first such attempts [1, 270, 271]. The model is based on the assumption that the undoped system is a quantum spin liquid. In such a state, all Cu spins would be paired into singlets in a manner such that the singlet-triplet spectrum is gapless. When a hole is introduced, one singlet is destroyed, yielding a free spinon; all other Cu spins still couple in singlet states. In such a picture, one would expect that the singlet-triplet excitations would dominate the magnetic excitation spectrum measured with neutrons; surprisingly, there has been little effort to make specific theoretical predictions of this spectrum for comparison with experiment. Instead, the analysis has been done in terms of electron-hole excitations [266]. As discussed above, such



a calculation has significant shortcomings when it comes to understanding underdoped cuprates.

Another alternative is a spiral spin-density wave, as has been proposed several times [272, 273, 274, 275]. A spiral state would be compatible with the incommensurate antiferromagnetic excitations at low energy [272, 274], and can also be used to model the full magnetic spectrum [275]. A look at the experimental record shows that a spiral phase cannot be the whole story. In the case of  $\text{La}_{1.875}\text{Ba}_{0.125}\text{CuO}_4$  and  $\text{La}_{1.6-x}\text{Nd}_{0.4}\text{Sr}_x\text{CuO}_4$ , where static magnetic order is observed, charge order is also found [276]. When there is charge order present, it follows that the spin-density modulation must have a collinear component in which the magnitude of the local moments is modulated [202]. There could also be a spiral component, but it is not essential. Furthermore, if holes simply cause a local rotation of the spin direction, then it is unclear why the ordering temperature of the Néel phase is so rapidly reduced by a small density of holes.

Given that stripe order is observed in certain cuprates (§8.5.2) and that the magnetic excitations of the stripe-ordered phase are consistent with the universal spectrum of good superconductors (Fig. 8.3), the simplest picture that is compatible with all of the data is to assume that charge stripes (dynamic ones in the case of the superconducting samples) are a common feature of the cuprates, at least on the underdoped side of the phase diagram. There is certainly plenty of theoretical motivation for stripes [277, 203, 278, 279], and the relevance of charge inhomogeneity to the superconducting mechanism is discussed in the chapter by Kivelson and Fradkin [280].

One surprising experimental observation is the minimal amount of damping of the magnetic excitations in underdoped cuprates, especially in the normal state. One would expect the continuum of electron-hole excitations to cause significant damping [90]. Could it be that the antiphase relationship of spin correlations across a charge stripe acts to separate the spin and charge excitations in a manner similar to that in a one-dimensional system [281, 282]? With over doping, there is evidence that regions of conventional electronic excitations become more significant. This is also the regime where magnetic excitations become weak. Could it be that the interaction of conventional electron-hole excitations with stripe-like patches causes a strong damping of the spin excitations? There is clearly plenty of work left to properly understand the cuprates.

## Acknowledgments

I am grateful to S. A. Kivelson and M. Hücker for critical comments. My work at Brookhaven is supported by the Office of Science, U.S. Department of Energy, under Contract No. DE-AC02-98CH10886.

## References

- [1] P. W. Anderson, *Science* **235**, 1169 (1987).
- [2] D. Vaknin, S. K. Sinha, D. E. Moncton, D. C. Johnston, J. M. Newsam, C. R. Safinya, and J. H. E. King, *Phys. Rev. Lett.* **58**, 2802 (1987).
- [3] M. A. Kastner, R. J. Birgeneau, G. Shirane, and Y. Endoh, *Rev. Mod. Phys.* **70**, 897 (1998).
- [4] P. Bourges, in *The Gap Symmetry and Fluctuations in High Temperature Superconductors*, edited by J. Bok, G. Deutscher, D. Pavuna, and S. A. Wolf (Plenum, New York, 1998), p. 349.
- [5] L. P. Regnault, P. Bourges, and P. Burlet, in *Neutron Scattering in Layered Copper-Oxide Superconductors*, edited by A. Furrer (Kluwer Academic, Dordrecht, 1998), pp. 85–134.
- [6] S. M. Hayden, in *Neutron Scattering in Layered Copper-Oxide Superconductors*, edited by A. Furrer (Kluwer Academic, Dordrecht, 1998), pp. 135–164.
- [7] T. E. Mason, in *Handbook on the Physics and Chemistry of Rare Earths, Vol. 31: High-Temperature Superconductors – II*, edited by J. K. A. Gschneidner, L. Eyring, and M. B. Maple (Elsevier, Amsterdam, 2001), pp. 281–314.
- [8] H. B. Brom and J. Zaanen, in *Handbook of Magnetic Materials, Vol. 15*, edited by K. H. J. Buschow (Elsevier Science, Amsterdam, 2003), pp. 379–496.
- [9] G. Shirane, S. M. Shapiro, and J. M. Tranquada, *Neutron Scattering with a Triple-Axis Spectrometer: Basic Techniques* (Cambridge University Press, Cambridge, 2002).
- [10] G. L. Squires, *Introduction to the Theory of Thermal Neutron Scattering* (Dover, Mineola, NY, 1996).
- [11] S.-W. Cheong, G. Aeppli, T. E. Mason, H. Mook, S. M. Hayden, P. C. Canfield, Z. Fisk, K. N. Clausen, and J. L. Martinez, *Phys. Rev. Lett.* **67**, 1791 (1991).
- [12] G. Aeppli, T. E. Mason, S. M. Hayden, H. A. Mook, and J. Kulda, *Science* **278**, 1432 (1997).
- [13] K. Yamada, C. H. Lee, K. Kurahashi, J. Wada, S. Wakimoto, S. Ueki, Y. Kimura, Y. Endoh, S. Hosoya, G. Shirane, et al., *Phys. Rev. B* **57**, 6165 (1998).
- [14] J. Rossat-Mignod, L. P. Regnault, C. Vettier, P. Bourges, P. Burlet, J. Bossy, J. Y. Henry, and G. Lapertot, *Physica B* **180&181**, 383 (1992).
- [15] H. A. Mook, M. Yethiraj, G. Aeppli, T. E. Mason, and T. Armstrong, *Phys. Rev. Lett.* **70**, 3490 (1993).
- [16] H. F. Fong, B. Keimer, D. Reznik, D. L. Milius, and I. A. Aksay, *Phys. Rev. B* **54**, 6708 (1996).
- [17] P. Dai, H. A. Mook, R. D. Hunt, and F. Doğan, *Phys. Rev. B* **63**, 054525 (2001).

- [18] Y. Sidis, S. Pailhès, B. Keimer, C. Ulrich, and L. P. Regnault, *Phys. Stat. Sol. (b)* **241**, 1204 (2004).
- [19] P. Bourges, Y. Sidis, H. F. Fong, B. Keimer, L. P. Regnault, J. Bossy, A. S. Ivanov, D. L. Milius, and I. A. Aksay, in *High Temperature Superconductivity*, edited by S. E. Barnes, J. Ashkenazi, J. L. Cohn, and F. Zuo (American Institute of Physics, Woodbury, NY, 1999), pp. 207–212.
- [20] H. F. Fong, P. Bourges, Y. Sidis, L. P. Regnault, A. Ivanov, G. D. Gu, N. Koshizuka, and B. Keimer, *Nature* **398**, 588 (1999).
- [21] J. Mesot, N. Metoki, M. Bohm, A. Hiess, and K. Kadowaki, *Physica C* **341**, 2105 (2000).
- [22] H. He, Y. Sidis, P. Bourges, G. D. Gu, A. Ivanov, N. Koshizuka, B. Liang, C. T. Lin, L. P. Regnault, E. Schoenherr, et al., *Phys. Rev. Lett.* **86**, 1610 (2001).
- [23] H. He, P. Bourges, Y. Sidis, C. Ulrich, L. P. Regnault, S. Pailhès, N. S. Berzigiarova, N. N. Kolesnikov, and B. Keimer, *Science* **295**, 1045 (2002).
- [24] M. Eschrig and M. R. Norman, *Phys. Rev. Lett.* **85**, 3261 (2000).
- [25] A. Abanov, A. V. Chubukov, and J. Schmalian, *J. Electron. Spectrosc. Relat. Phenom.* **117–118**, 129 (2001).
- [26] H.-Y. Kee, S. A. Kivelson, and G. Aeppli, *Phys. Rev. Lett.* **88**, 257002 (2002).
- [27] S. M. Hayden, H. A. Mook, P. Dai, T. G. Perring, and F. Doğan, *Nature* **429**, 531 (2004).
- [28] C. Stock, W. J. L. Buyers, R. A. Cowley, P. S. Clegg, R. Coldea, C. D. Frost, R. Liang, D. Peets, D. Bonn, W. N. Hardy, et al., *Phys. Rev. B* **71**, 024522 (2005).
- [29] V. Hinkov, S. Pailhès, P. Bourges, Y. Sidis, A. Ivanov, A. Kulakov, C. T. Lin, D. P. Chen, C. Bernhard, and B. Keimer, *Nature* **430**, 650 (2004).
- [30] P. Bourges, H. F. Fong, L. P. Regnault, J. Bossy, C. Vettier, D. L. Milius, I. A. Aksay, and B. Keimer, *Phys. Rev. B* **56**, R11 439 (1997).
- [31] P. Dai, H. A. Mook, S. M. Hayden, G. Aeppli, T. G. Perring, R. D. Hunt, and F. Doğan, *Science* **284**, 1344 (1999).
- [32] S. M. Hayden, G. Aeppli, T. G. Perring, H. A. Mook, and F. Doğan, *Phys. Rev. B* **54**, R6905 (1996).
- [33] D. Reznik, P. Bourges, H. F. Fong, L. P. Regnault, J. Bossy, C. Vettier, D. L. Milius, I. A. Aksay, and B. Keimer, *Phys. Rev. B* **53**, R14741 (1996).
- [34] H. A. Mook, P. Dai, S. M. Hayden, G. Aeppli, T. G. Perring, and F. Doğan, *Nature* **395**, 580 (1998).
- [35] M. Arai, T. Nishijima, Y. Endoh, T. Egami, S. Tajima, K. Tomimoto, Y. Shiohara, M. Takahashi, A. Garrett, and S. M. Bennington, *Phys. Rev. Lett.* **83**, 608 (1999).
- [36] P. Bourges, Y. Sidis, H. F. Fong, L. P. Regnault, J. Bossy, A. Ivanov, and B. Keimer, *Science* **288**, 1234 (2000).

- [37] S. Pailhès, Y. Sidis, P. Bourges, V. Hinkov, A. Ivanov, C. Ulrich, L. P. Regnault, and B. Keimer, *Phys. Rev. Lett.* **93**, 167001 (2004).
- [38] D. Reznik, P. Bourges, L. Pintschovius, Y. Endoh, Y. Sidis, T. Matsui, and S. Tajima, *Phys. Rev. Lett.* **93**, 207003 (2004).
- [39] M. Ito, H. Harashina, Y. Yasui, M. Kanada, S. Iikubo, M. Sato, A. Kobayashi, and K. Kakurai, *J. Phys. Soc. Japan* **71**, 265 (2002).
- [40] N. B. Christensen, D. F. McMorrow, H. M. Rønnow, B. Lake, S. M. Hayden, G. Aeppli, T. G. Perring, M. Mangkorntong, M. Nohara, and H. Tagaki, *Phys. Rev. Lett.* **93**, 147002 (2004).
- [41] M. Fujita, H. Goka, K. Yamada, J. M. Tranquada, and L. P. Regnault, *Phys. Rev. B* **70**, 104517 (2004).
- [42] J. M. Tranquada, H. Woo, T. G. Perring, H. Goka, G. D. Gu, G. Xu, M. Fujita, and K. Yamada, *Nature* **429**, 534 (2004).
- [43] J. M. Tranquada, B. J. Sternlieb, J. D. Axe, Y. Nakamura, and S. Uchida, *Nature* **375**, 561 (1995).
- [44] J. M. Tranquada, H. Woo, T. G. Perring, H. Goka, G. D. Gu, G. Xu, M. Fujita, and K. Yamada, *cond-mat/0411082*.
- [45] T. Barnes and J. Riera, *Phys. Rev. B* **50**, 6817 (1994).
- [46] H. A. Mook, P. Dai, F. Doğan, and R. D. Hunt, *Nature* **404**, 729 (2000).
- [47] C. Stock, W. J. L. Buyers, R. Liang, D. Peets, Z. Tun, D. Bonn, W. N. Hardy, and R. J. Birgeneau, *Phys. Rev. B* **69**, 014502 (2004).
- [48] B. Lake, G. Aeppli, T. E. Mason, A. Schröder, D. F. McMorrow, K. Lefmann, M. Isshiki, M. Nohara, H. Takagi, and S. M. Hayden, *Nature* **400**, 43 (1999).
- [49] J. P. Lu, *Phys. Rev. Lett.* **68**, 125 (1992).
- [50] P. Dai, H. A. Mook, G. Aeppli, S. M. Hayden, and F. Doğan, *Nature* **406**, 965 (2000).
- [51] J. M. Tranquada, C. H. Lee, K. Yamada, Y. S. Lee, L. P. Regnault, and H. M. Rønnow, *Phys. Rev. B* **69**, 174507 (2004).
- [52] B. Lake, G. Aeppli, K. N. Clausen, D. F. McMorrow, K. Lefmann, N. E. Hussey, N. Mangkorntong, M. Nohara, H. Takagi, T. E. Mason, et al., *Science* **291**, 1759 (2001).
- [53] P. W. Anderson, *Adv. Phys.* **46**, 3 (1997).
- [54] J. M. Tranquada, A. H. Moudden, A. I. Goldman, P. Zolliker, D. E. Cox, G. Shirane, S. K. Sinha, D. Vaknin, D. C. Johnston, M. S. Alvarez, et al., *Phys. Rev. B* **38**, 2477 (1988).
- [55] Y. S. Lee, R. J. Birgeneau, M. A. Kastner, Y. Endoh, S. Wakimoto, K. Yamada, R. W. Erwin, S.-H. Lee, and G. Shirane, *Phys. Rev. B* **60**, 3643 (1999).
- [56] J. M. Tranquada, D. E. Cox, W. Kunnmann, H. Moudden, G. Shirane, M. Suenaga, P. Zolliker, D. Vaknin, S. K. Sinha, M. S. Alvarez, et al., *Phys. Rev. Lett.* **60**, 156 (1988).
- [57] T. Freltoft, J. E. Fischer, G. Shirane, D. E. Moncton, S. K. Sinha, D. Vaknin, J. P. Remeikas, A. S. Cooper, and D. Harshman, *Phys. Rev. B* **36**, 826 (1987).

- [58] M. A. Kastner, R. J. Birgeneau, T. R. Thurston, P. J. Picone, H. P. Jensen, D. R. Gabbe, M. Sato, K. Fukuda, S. Shamoto, Y. Endoh, et al., *Phys. Rev. B* **38**, 6636 (1988).
- [59] T. Thio and A. Aharony, *Phys. Rev. Lett.* **73**, 894 (1994).
- [60] A. Zheludev, S. Maslov, I. Zaliznyak, L. P. Regnault, T. Masuda, K. Uchinokura, R. Erwin, and G. Shirane, *Phys. Rev. Lett.* **81**, 5410 (1998).
- [61] D. Coffey, T. M. Rice, and F. C. Zhang, *Phys. Rev. B* **44**, 10112 (1991).
- [62] J. Stein, O. Entin-Wohlman, and A. Aharony, *Phys. Rev. B* **53**, 775 (1996).
- [63] B. O. Wells, Y. S. Lee, M. A. Kastner, R. J. Christianson, R. J. Birgeneau, K. Yamada, Y. Endoh, and G. Shirane, *Science* **277**, 1067 (1997).
- [64] B. Keimer, A. Aharony, A. Auerbach, R. J. Birgeneau, A. Cassanho, Y. Endoh, R. W. Erwin, M. A. Kastner, and G. Shirane, *Phys. Rev. B* **45**, 7430 (1992).
- [65] K. Yamada, E. Kudo, Y. Endoh, Y. Hidaka, M. Oda, M. Suzuki, and T. Murakami, *Solid State Commun.* **64**, 753 (1987).
- [66] T. Yildirim, A. B. Harris, O. Entin-Wohlman, and A. Aharony, *Phys. Rev. Lett.* **72**, 3710 (1994).
- [67] T. Yildirim, A. B. Harris, O. Entin-Wohlman, and A. Aharony, *Phys. Rev. Lett.* **73**, 2919 (1994).
- [68] R. Coldea, S. M. Hayden, G. Aeppli, T. G. Perring, C. D. Frost, T. E. Mason, S.-W. Cheong, and Z. Fisk, *Phys. Rev. Lett.* **86**, 5377 (2001).
- [69] D. Vaknin, S. K. Sinha, C. Stassis, L. L. Miller, and D. C. Johnston, *Phys. Rev. B* **41**, 1926 (1990).
- [70] M. Greven, R. J. Birgeneau, Y. Endoh, M. A. Kastner, M. Matsuda, and G. Shirane, *Z. Phys. B* **96**, 465 (1995).
- [71] Y. Tokura, S. Koshihara, T. Arima, H. Takagi, S. Ishibashi, T. Ido, and S. Uchida, *Phys. Rev. B* **41**, 11657 (1990).
- [72] D. Vaknin, L. L. Miller, and J. L. Zarestky, *Phys. Rev. B* **56**, 8351 (1997).
- [73] M. Matsuda, K. Yamada, K. Kakurai, H. Kadowaki, T. R. Thurston, Y. Endoh, Y. Hidaka, R. J. Birgeneau, M. A. Kastner, P. M. Gehring, et al., *Phys. Rev. B* **42**, 10098 (1990).
- [74] S. Skanthakumar, J. W. Lynn, J. L. Peng, and Z. Y. Li, *Phys. Rev. B* **47**, 6173 (1993).
- [75] J. W. Lynn and S. Skanthakumar, in *Handbook on the Physics and Chemistry of Rare Earths, Vol. 31*, edited by J. K. A. Gschneidner, L. Eyring, and M. B. Maple (Elsevier Science, Amsterdam, 2001), pp. 315–350.
- [76] P. Bourges, H. Casalta, A. S. Ivanov, and D. Petitgrand, *Phys. Rev. Lett.* **79**, 4906 (1997).
- [77] I. W. Sumarlin, J. W. Lynn, T. Chattopadhyay, S. N. Barilo, D. I. Zhigunov, and J. L. Peng, *Phys. Rev. B* **51**, 5824 (1995).

- [78] H. Casalta, P. Schleger, E. Brecht, W. Montfrooij, N. H. Andersen, B. Lebech, W. W. Schmahl, H. Fuess, R. Liang, W. N. Hardy, et al., *Phys. Rev. B* **50**, 9688 (1994).
- [79] J. Mizuki, Y. Kubo, T. Manako, Y. Shimakawa, H. Igarashi, J. M. Tranquada, Y. Fujii, L. Rebelsky, and G. Shirane, *Physica C* **156**, 781 (1988).
- [80] D. Vaknin, E. Caignol, P. K. Davies, J. E. Fischer, D. C. Johnston, and D. P. Goshorn, *Phys. Rev. B* **39**, 9122 (1989).
- [81] R. Sachidanandam, T. Yildirim, A. B. Harris, A. Aharony, and O. Entin-Wohlman, *Phys. Rev. B* **56**, 260 (1997).
- [82] D. Petitgrand, S. V. Maleyev, P. Bourges, and A. S. Ivanov, *Phys. Rev. B* **59**, 1079 (1999).
- [83] P. Burllet, J. Y. Henry, and L. P. Regnault, *Physica C* **296**, 205 (1998).
- [84] A. Jánossy, F. Simon, T. Fehér, A. Rockenbauer, L. Korecz, C. Chen, A. J. S. Chowdhury, and J. W. Hodby, *Phys. Rev. B* **59**, 1176 (1999).
- [85] H. Kadowaki, M. Nishi, Y. Yamada, H. Takeya, H. Takei, S. M. Shapiro, and G. Shirane, *Phys. Rev. B* **37**, 7932 (1988).
- [86] E. Brecht, W. W. Schmahl, H. Fuess, H. Casalta, P. Schleger, B. Lebech, N. H. Andersen, and T. Wolf, *Phys. Rev. B* **52**, 9601 (1995).
- [87] N. H. Andersen and G. Uimin, *Phys. Rev. B* **56**, 10840 (1997).
- [88] S. Shamoto, M. Sato, J. M. Tranquada, B. J. Sternlieb, and G. Shirane, *Phys. Rev. B* **48**, 13817 (1993).
- [89] M. E. Lines, *J. Phys. Chem. Solids* **31**, 101 (1970).
- [90] J. Lorenzana, G. Seibold, and R. Coldea (2005), [cond-mat/0507131](#).
- [91] L. Capriotta, A. Läuchli, and A. Paramekanti (2005), [cond-mat/0406188](#).
- [92] C. Yasuda, S. Todo, K. Hukushima, F. Alet, M. Keller, M. Troyer, and H. Takayama, *Phys. Rev. Lett.* **94**, 217201 (2005).
- [93] K. M. Kojima, Y. Fudamoto, M. Larkin, G. M. Luke, J. Merrin, B. Nachumi, Y. J. Uemura, N. Motoyama, H. Eisaki, S. Uchida, et al., *Phys. Rev. Lett.* **78**, 1787 (1997).
- [94] P. W. Anderson, *Phys. Rev.* **115**, 2 (1959).
- [95] T. Oguchi, *Phys. Rev.* **117**, 117 (1960).
- [96] R. R. P. Singh, *Phys. Rev. B* **39**, 9760 (1989).
- [97] K. B. Lyons, P. A. Fleury, J. P. Remeika, A. S. Cooper, and T. J. Negran, *Phys. Rev. B* **37**, 2353 (1988).
- [98] V. J. Emery and G. Reiter, *Phys. Rev. B* **38**, 4547 (1988).
- [99] A. B. Van Oosten, R. Broer, and W. C. Nieupoort, *Chem. Phys. Lett.* **257**, 207 (1996).
- [100] D. Muñoz, F. Illas, and I. P. R. Moreira, *Phys. Rev. Lett.* **84**, 1579 (2000).
- [101] I. A. Zaliznyak, H. Woo, T. G. Perring, C. L. Broholm, C. D. Frost, and H. Takagi, *Phys. Rev. Lett.* **93**, 087202 (2004).
- [102] M. Takahashi, *J. Phys. C* **10**, 1289 (1977).
- [103] M. Roger and J. M. Delrieu, *Phys. Rev. B* **39**, 2299 (1989).

- [104] A. H. MacDonald, S. M. Girvin, and D. Yoshioka, *Phys. Rev. B* **37**, 9753 (1988).
- [105] D. K. Morr, *Phys. Rev. B* **58**, R587 (1998).
- [106] J. F. Annett, R. M. Martin, A. K. McMahan, and S. Satpathy, *Phys. Rev. B* **40**, 2620 (1989).
- [107] J. M. Tranquada, G. Shirane, B. Keimer, S. Shamoto, and M. Sato, *Phys. Rev. B* **40**, 4503 (1989).
- [108] J. D. Jorgensen, B. W. Veal, A. P. Paulikas, L. J. Nowicki, G. W. Crabtree, H. Claus, and W. K. Kwok, *Phys. Rev. B* **41**, 1863 (1990).
- [109] E. F. Shender, *Sov. Phys. JETP* **56** (1982).
- [110] B. Keimer, R. J. Birgeneau, A. Cassanho, Y. Endoh, M. Greven, M. A. Kastner, and G. Shirane, *Z. Phys. B* **91**, 373 (1993).
- [111] C. J. Peters, R. J. Birgeneau, M. A. Kastner, H. Yoshizawa, Y. Endoh, J. Tranquada, G. Shirane, Y. Hidaka, M. Oda, M. Suzuki, et al., *Phys. Rev. B* **37**, 9761 (1988).
- [112] L. Shekhtman, O. Entin-Wohlman, and A. Aharony, *Phys. Rev. Lett.* **69**, 836 (1992).
- [113] C. Vettier, P. Burlet, J. Y. Henry, M. J. Jurgens, G. Lapertot, L. P. Regnault, and J. Rossat-Mignod, *Physica Scripta* **T29**, 110 (1989).
- [114] J. Rossat-Mignod, L. P. Regnault, M. J. Jurgens, C. Vettier, P. Burlet, J. Y. Henry, and G. Lapertot, *Physica B* **163**, 4 (1990).
- [115] G. Shirane, Y. Endoh, R. J. Birgeneau, M. A. Kastner, Y. Hidaka, M. Oda, M. Suzuki, and T. Murakami, *Phys. Rev. Lett.* **59**, 1613 (1987).
- [116] R. J. Birgeneau, M. Greven, M. A. Kastner, Y. S. Lee, B. O. Wells, Y. Endoh, K. Yamada, and G. Shirane, *Phys. Rev. B* **59**, 13788 (1999).
- [117] M. Greven, R. J. Birgeneau, Y. Endoh, M. A. Kastner, B. Keimer, M. Matsuda, G. Shirane, and T. R. Thurston, *Phys. Rev. Lett.* **72**, 1096 (1994).
- [118] S. Chakravarty, B. I. Halperin, and D. R. Nelson, *Phys. Rev. B* **39**, 2344 (1989).
- [119] P. Hasenfratz and F. Niedermayer, *Phys. Lett. B* **268**, 231 (1991).
- [120] S. Chakravarty, B. I. Halperin, and D. R. Nelson, *Phys. Rev. Lett.* **60**, 1057 (1988).
- [121] B. J. Suh, F. Borsa, L. L. Miller, M. Corti, D. C. Johnston, and D. R. Torgeson, *Phys. Rev. Lett.* **75**, 2212 (1995).
- [122] A. Cuccoli, T. Roscilde, R. Vaia, and P. Verrucchi, *Phys. Rev. Lett.* **90**, 167205 (2003).
- [123] Y. J. Kim, R. J. Birgeneau, F. C. Chou, R. W. Erwin, and M. A. Kastner, *Phys. Rev. Lett.* **86**, 3144 (2001).
- [124] P. C. Hohenberg and B. I. Halperin, *Rev. Mod. Phys.* **49**, 435 (1977).
- [125] C. Niedermayer, C. Bernhard, T. Blasius, A. Golnik, A. Moodenbaugh, and J. I. Budnick, *Phys. Rev. Lett.* **80**, 3843 (1998).
- [126] O. P. Vajk, P. K. Mang, M. Greven, P. M. Gehring, and J. W. Lynn, *Science* **295**, 1691 (2002).

- [127] M. Matsuda, M. Fujita, K. Yamada, R. J. Birgeneau, Y. Endoh, and G. Shirane, *Phys. Rev. B* **65**, 134515 (2002).
- [128] S. Wakimoto, R. J. Birgeneau, M. A. Kastner, Y. S. Lee, R. Erwin, P. M. Gehring, S. H. Lee, M. Fujita, K. Yamada, Y. Endoh, et al., *Phys. Rev. B* **61**, 3699 (2000).
- [129] M. Matsuda, M. Fujita, K. Yamada, R. J. Birgeneau, M. A. Kastner, H. Hiraka, Y. Endoh, S. Wakimoto, and G. Shirane, *Phys. Rev. B* **62**, 9148 (2000).
- [130] S. Wakimoto, R. J. Birgeneau, Y. S. Lee, and G. Shirane, *Phys. Rev. B* **63**, 172501 (2001).
- [131] M. Fujita, K. Yamada, H. Hiraka, P. M. Gehring, S. H. Lee, S. Wakimoto, and G. Shirane, *Phys. Rev. B* **65**, 064505 (2002).
- [132] F. C. Chou, N. R. Belk, M. A. Kastner, R. J. Birgeneau, and A. Aharony, *Phys. Rev. Lett.* **75**, 2204 (1995).
- [133] S. Wakimoto, S. Ueki, Y. Endoh, and K. Yamada, *Phys. Rev. B* **62**, 3547 (2000).
- [134] J. M. Tranquada, in *Neutron Scattering in Layered Copper-Oxide Superconductors*, edited by A. Furrer (Kluwer, Dordrecht, The Netherlands, 1998), p. 225.
- [135] J. D. Jorgensen, B. Dabrowski, S. Pei, D. G. Hinks, L. Soderholm, B. Morosin, J. E. Schirber, E. L. Venturini, and D. S. Ginley, *Phys. Rev. B* **38**, 11337 (1988).
- [136] P. C. Hammel, A. P. Reyes, Z. Fisk, M. Takigawa, J. D. Thompson, R. H. Heffner, S.-W. Cheong, and J. E. Schirber, *Phys. Rev. B* **42**, 6781 (1990).
- [137] V. P. Gnezdilov, Y. G. Pashkevich, J. M. Tranquada, P. Lemmens, G. Gntherodt, A. V. Yeremenko, S. N. Barilo, S. V. Shiryayev, L. A. Kurnevich, and P. M. Gehring, *Phys. Rev. B* **69**, 174508 (2004).
- [138] A. Renault, J. K. Burdett, and J.-P. Pouget, *J. Solid State Chem.* **71**, 587 (1987).
- [139] H. Maletta, E. Pörschke, B. Rupp, and P. Meuffels, *Z. Phys. B* **77**, 181 (1989).
- [140] R. J. Cava, A. W. Hewat, E. A. Hewat, B. Batlogg, M. Marezio, K. M. Rabe, J. J. Krajewski, J. W. F. Peck, and J. L. W. Rupp, *Physica C* **165**, 419 (1990).
- [141] G. Uimin and J. Rossat-Mignod, *Physica C* **199**, 251 (1992).
- [142] J. Rossat-Mignod, P. Burlet, M. J. Jurgens, C. Vettier, L. P. Regnault, J. Y. Henry, C. Ayache, L. Forro, H. Noel, M. Potel, et al., *J. Phys. (Paris)* **49**, C8 (1988).
- [143] C. Stock, W. J. L. Buyers, Z. Yamani, C. L. Broholm, J.-H. Chung, Z. Tun, R. Liang, D. Bonn, W. N. Hardy, and R. J. Birgeneau (2005), [cond-mat/0505083](#).
- [144] C. Ulrich, S. Kondo, M. Reehuis, H. He, C. Bernhard, C. Niedermayer, F. Bourée, P. Bourges, M. Ohl, H. M. Rønnow, et al., *Phys. Rev. B* **65**, 220507 (2002).



- [145] M. Hücker, Y.-J. Kim, G. D. Gu, J. M. Tranquada, B. D. Gaulin, and J. W. Lynn, *Phys. Rev. B* **71**, 094510 (2005).
- [146] N. L. Wang, P. Zheng, T. Feng, G. D. Gu, C. C. Homes, J. M. Tranquada, B. D. Gaulin, and T. Timusk, *Phys. Rev. B* **67**, 134526 (2003).
- [147] R. J. Cava, B. Batlogg, T. T. Palstra, J. J. Krajewski, W. F. P. Jr., A. P. Ramirez, and L. W. R. Jr., *Phys. Rev. B* **43**, 1229 (1991).
- [148] S. Shinomori, Y. Okimoto, M. Kawasaki, and Y. Tokura, *J. Phys. Soc. Japan* **71**, 705 (2002).
- [149] S.-W. Cheong, H. Y. Hwang, C. H. Chen, B. Batlogg, J. L. W. Rupp, and S. A. Carter, *Phys. Rev. B* **49**, 7088 (1994).
- [150] H. Yoshizawa, T. Kakeshita, R. Kajimoto, T. Tanabe, T. Katsufuji, and Y. Tokura, *Phys. Rev. B* **61**, R854 (2000).
- [151] J. M. Tranquada, D. J. Buttrey, V. Sachan, and J. E. Lorenzo, *Phys. Rev. Lett.* **73**, 1003 (1994).
- [152] V. Sachan, D. J. Buttrey, J. M. Tranquada, J. E. Lorenzo, and G. Shirane, *Phys. Rev. B* **51**, 12742 (1995).
- [153] J. M. Tranquada, D. J. Buttrey, and V. Sachan, *Phys. Rev. B* **54**, 12318 (1996).
- [154] P. Wochner, J. M. Tranquada, D. J. Buttrey, and V. Sachan, *Phys. Rev. B* **57**, 1066 (1998).
- [155] K. Yamada, T. Omata, K. Nakajima, S. Hosoya, T. Sumida, and Y. Endoh, *Physica C* **191**, 15 (1992).
- [156] J. M. Tranquada, Y. Kong, J. E. Lorenzo, D. J. Buttrey, D. E. Rice, and V. Sachan, *Phys. Rev. B* **50**, 6340 (1994).
- [157] J. M. Tranquada, J. E. Lorenzo, D. J. Buttrey, and V. Sachan, *Phys. Rev. B* **52**, 3581 (1995).
- [158] J. Li, Y. Zhu, J. M. Tranquada, K. Yamada, and D. J. Buttrey, *Phys. Rev. B* **67**, 012404 (2003).
- [159] Y. Yoshinari, P. C. Hammel, and S.-W. Cheong, *Phys. Rev. Lett.* **82**, 3536 (1999).
- [160] I. M. Abu-Shiekh, O. O. Bernal, A. A. Menovsky, H. B. Brom, and J. Zaanen, *Phys. Rev. Lett.* **83**, 3309 (1999).
- [161] S.-H. Lee and S.-W. Cheong, *Phys. Rev. Lett.* **79**, 2514 (1997).
- [162] K. Ishizaka, T. Arima, Y. Murakami, R. Kajimoto, H. Yoshizawa, N. Nagao, and Y. Tokura, *Phys. Rev. Lett.* **92**, 196404 (2004).
- [163] P. Bourges, Y. Sidis, M. Braden, K. Nakajima, and J. M. Tranquada, *Phys. Rev. Lett.* **90**, 147202 (2003).
- [164] A. T. Boothroyd, D. Prabhakaran, P. G. Freeman, S. J. S. Lister, M. Enderle, A. Hiess, and J. Kulda, *Phys. Rev. B* **67**, 100407(R) (2003).
- [165] H. Woo, A. T. Boothroyd, K. Nakajima, T. G. Perring, C. D. Frost, P. G. Freeman, D. Prabhakaran, K. Yamada, and J. M. Tranquada, *Phys. Rev. B* **72**, 064437 (2005).
- [166] K. Yamada, M. Arai, Y. Endoh, S. Hosoya, K. Nakajima, T. Perring, and A. Taylor, *J. Phys. Soc. Jpn.* **60**, 1197 (1991).

- [167] A. T. Boothroyd, P. G. Freeman, D. Prabhakaran, A. Hiess, M. Enderle, J. Kulda, and F. Altorfer, *Phys. Rev. Lett.* **91**, 257201 (2003).
- [168] S.-H. Lee, J. M. Tranquada, K. Yamada, D. J. Buttrey, Q. Li, and S.-W. Cheong, *Phys. Rev. Lett.* **88**, 126401 (2002).
- [169] T. Katsufuji, T. Tanabe, T. Ishikawa, Y. Fukuda, T. Arima, and Y. Tokura, *Phys. Rev. B* **54**, R14230 (1996).
- [170] C. C. Homes, J. M. Tranquada, Q. Li, A. R. Moodenbaugh, and D. J. Buttrey, *Phys. Rev. B* **67**, 184516 (2003).
- [171] J. M. Tranquada, *J. Phys. Chem. Solids* **59**, 2150 (1998).
- [172] N. Ichikawa, S. Uchida, J. M. Tranquada, T. Niemöller, P. M. Gehring, S.-H. Lee, and J. R. Schneider, *Phys. Rev. Lett.* **85**, 1738 (2000).
- [173] J. D. Axe and M. K. Crawford, *J. Low Temp. Phys.* **95**, 271 (1994).
- [174] M. Fujita, H. Goka, K. Yamada, and M. Matsuda, *Phys. Rev. Lett.* **88**, 167008 (2002).
- [175] M. Fujita, H. Goka, K. Yamada, and M. Matsuda, *Phys. Rev. B* **66**, 184503 (2002).
- [176] H. Kimura, H. Goka, M. Fujita, Y. Noda, K. Yamada, and N. Ikeda, *Phys. Rev. B* **67**, 140503(R) (2003).
- [177] B. V. Fine, *Phys. Rev. B* **70**, 224508 (2004).
- [178] J. M. Tranquada, N. Ichikawa, K. Kakurai, and S. Uchida, *J. Phys. Chem. Solids* **60**, 1019 (1999).
- [179] M. v. Zimmermann, A. Vigliante, T. Niemöller, N. Ichikawa, T. Frello, S. Uchida, N. H. Andersen, J. Madsen, P. Wochner, J. M. Tranquada, et al., *Europhys. Lett.* **41**, 629 (1998).
- [180] H. A. Mook, P. Dai, and F. Doğan, *Phys. Rev. Lett.* **88**, 097004 (2002).
- [181] S. Sanna, G. Allodi, G. Concas, A. D. Hillier, and R. D. Renzi, *Phys. Rev. Lett.* **93**, 207001 (2004).
- [182] A. T. Savici, Y. Fudamoto, I. M. Gat, T. Ito, M. I. Larkin, Y. J. Uemura, G. M. Luke, K. M. Kojima, Y. S. Lee, M. A. Kastner, et al., *Phys. Rev. B* **66**, 014524 (2002).
- [183] C. D. Batista, G. Ortiz, and A. V. Balatsky, *Phys. Rev. B* **64**, 172508 (2001).
- [184] F. Krüger and S. Scheidl, *Phys. Rev. B* **67**, 134512 (2003).
- [185] E. W. Carlson, D. X. Yao, and D. K. Campbell, *Phys. Rev. B* **70**, 064505 (2004).
- [186] M. Vojta and T. Ulbricht, *Phys. Rev. Lett.* **93**, 127002 (2004).
- [187] G. S. Uhrig, K. P. Schmidt, and M. Grüninger, *Phys. Rev. Lett.* **93**, 267003 (2004).
- [188] G. Seibold and J. Lorenzana, *Phys. Rev. Lett.* **94**, 107006 (2005).
- [189] M. Ito, Y. Yasui, S. Iikubo, M. Sato, A. Kobayashi, and K. Kakurai, *J. Phys. Soc. Japan* **72**, 1627 (2003).
- [190] E. Fawcett, H. L. Alberts, V. Y. Galkin, D. R. Noakes, and J. V. Yakhmi, *Rev. Mod. Phys.* **66**, 25 (1994).
- [191] E. Fawcett, *Rev. Mod. Phys.* **60**, 209 (1988).
- [192] A. W. Overhauser and A. Arrott, *Phys. Rev. Lett.* **4**, 226 (1960).

- [193] W. M. Lomer, Proc. Phys. Soc. London **80**, 489 (1962).
- [194] S. K. Sinha, G. R. Kline, C. Stassis, N. Chesser, and N. Wakabayashi, Phys. Rev. B **15**, 1415 (1977).
- [195] T. Fukuda, Y. Endoh, K. Yamada, M. Takeda, S. Itoh, M. Arai, and T. Otomo, J. Phys. Soc. Japan **65**, 1418 (1996).
- [196] E. Kaneshita, M. Ichioka, and K. Machida, J. Phys. Soc. Jpn. **70**, 866 (2001).
- [197] R. S. Fishman and S. H. Liu, Phys. Rev. Lett. **76**, 2398 (1996).
- [198] S. M. Hayden, R. Doubble, G. Aeppli, T. G. Perring, and E. Fawcett, Phys. Rev. Lett. **84**, 999 (2000).
- [199] J. B. Staunton, J. Poulter, B. Ginatempo, E. Bruno, and D. D. Johnson, Phys. Rev. Lett. **82**, 3340 (1999).
- [200] R. Pynn, W. Press, S. M. Shapiro, and S. A. Werner, Phys. Rev. B **13**, 295 (1976).
- [201] J. M. Tranquada, J. D. Axe, N. Ichikawa, Y. Nakamura, S. Uchida, and B. Nachumi, Phys. Rev. B **54**, 7489 (1996).
- [202] O. Zachar, S. A. Kivelson, and V. J. Emery, Phys. Rev. B **57**, 1422 (1998).
- [203] S. A. Kivelson, I. P. Bindloss, E. Fradkin, V. Oganesyan, J. M. Tranquada, A. Kapitulnik, and C. Howald, Rev. Mod. Phys. **75**, 1201 (2003).
- [204] S. Chakravarty, R. B. Laughlin, D. K. Morr, and C. Nayak, Phys. Rev. B **63**, 094503 (2001).
- [205] X.-G. Wen and P. A. Lee, Phys. Rev. Lett. **76**, 503 (1996).
- [206] H. A. Mook, P. C. Dai, S. M. Hayden, A. Hiess, J. W. Lynn, S.-H. Lee, and F. Doğan, Phys. Rev. B **66**, 144513 (2002).
- [207] C. Stock, W. J. L. Buyers, Z. Tun, R. Liang, D. Peets, D. Bonn, W. N. Hardy, and L. Taillefer, Phys. Rev. B **66**, 024505 (2002).
- [208] H. A. Mook, P. C. Dai, S. M. Hayden, A. Hiess, S.-H. Lee, and F. Doğan, Phys. Rev. B **69**, 134509 (2004).
- [209] C. M. Varma, Phys. Rev. B **55**, 14554 (1997).
- [210] S.-H. Lee, C. F. Majkrzak, S. K. Sinha, C. Stassis, H. Kawano, G. H. Lander, P. J. Brown, H. F. Fong, S.-W. Cheong, H. Matsushita, et al., Phys. Rev. B **60**, 10405 (1999).
- [211] M. E. Simon and C. M. Varma, Phys. Rev. Lett. **89**, 247003 (2002).
- [212] B. Fauqué, Y. Sidis, V. Hinkov, S. Pailhès, C. T. Lin, X. Chaud, and P. Bourges (2005), [cond-mat/0509210](#).
- [213] S. Wakimoto, H. Zhang, K. Yamada, I. Swainson, H. Kim, and R. J. Birgeneau, Phys. Rev. Lett. **92**, 217004 (2004).
- [214] A. V. Balatsky and P. Bourges, Phys. Rev. Lett. **82**, 5337 (1999).
- [215] H. Hiraka, Y. Endoh, M. Fujita, Y. S. Lee, J. Kulda, A. Ivanov, and R. J. Birgeneau, J. Phys. Soc. Japan **70**, 853 (2001).
- [216] T. Nakano, N. Momono, M. Oda, and M. Ido, J. Phys. Soc. Japan **67**, 2622 (1998).
- [217] T. Kato, S. Okitsu, and H. Sakata, Phys. Rev. B **72**, 144518 (2005).

- [218] A. Ino, C. Kim, M. Nakamura, T. Yoshida, T. Mizokawa, Z.-X. Shen, A. Fujimori, T. Kakeshita, H. Eisaki, and S. Uchida, *Phys. Rev. B* **65**, 094504 (2002).
- [219] C.-H. Lee, K. Yamada, Y. Endoh, G. Shirane, R. J. Birgeneau, M. A. Kastner, M. Greven, and Y.-J. Kim, *J. Phys. Soc. Japan* **69**, 1170 (2000).
- [220] C. H. Lee, K. Yamada, H. Hiraka, C. R. Venkateswara Rao, and Y. Endoh, *Phys. Rev. B* **67**, 134521 (2003).
- [221] P. Bourges, H. Casalta, L. P. Regnault, J. Bossy, P. Burlet, C. Vettier, E. Beaugnon, P. Gautier-Picard, and R. Tournier, *Physica B* **234-236**, 830 (1997).
- [222] Y. Ando and K. Segawa, *Phys. Rev. Lett.* **88**, 167005 (2002).
- [223] S. Katano, M. Sato, K. Yamada, T. Suzuki, and T. Fukase, *Phys. Rev. B* **62**, R14677 (2000).
- [224] B. Lake, H. M. Rønnow, N. B. Christensen, G. Aeppli, K. Lefmann, D. F. McMorrow, P. Vorderwisch, P. Smeibidl, N. Mangkorntong, T. Sasagawa, et al., *Nature* **415**, 299 (2002).
- [225] E. Demler, S. Sachdev, and Y. Zhang, *Phys. Rev. Lett.* **87**, 067202 (2001).
- [226] S. A. Kivelson, D.-H. Lee, E. Fradkin, and V. Oganesyan, *Phys. Rev. B* **66**, 144516 (2002).
- [227] B. Khaykovich, Y. S. Lee, R. W. Erwin, S.-H. Lee, S. Wakimoto, K. J. Thomas, M. A. Kastner, and R. J. Birgeneau, *Phys. Rev. B* **66**, 014528 (2002).
- [228] B. Khaykovich, R. J. Birgeneau, F. C. Chou, R. W. Erwin, M. A. Kastner, S.-H. Lee, Y. S. Lee, P. Smeibidl, P. Vorderwisch, and S. Wakimoto, *Phys. Rev. B* **67**, 054501 (2003).
- [229] J. E. Hoffman, E. W. Hudson, K. M. Lang, V. Madhavan, H. Eisaki, S. Uchida, and J. C. Davis, *Science* **295**, 466 (2002).
- [230] B. Khaykovich, S. Wakimoto, R. J. Birgeneau, M. A. Kastner, Y. S. Lee, P. Smeibidl, P. Vorderwisch, and K. Yamada, *Phys. Rev. B* **71**, 220508(R) (2005).
- [231] S. Wakimoto, R. J. Birgeneau, Y. Fujimaki, N. Ichikawa, T. Kasuga, Y. J. Kim, K. M. Kojima, S.-H. Lee, H. Niko, J. M. Tranquada, et al., *Phys. Rev. B* **67**, 184419 (2003).
- [232] T. Suzuki, T. Goto, K. Chiba, T. Shinoda, T. Fukase, H. Kimura, K. Yamada, M. Ohashi, and Y. Yamaguchi, *Phys. Rev. B* **57**, R3229 (1998).
- [233] Y. Horibe, Y. Inoue, and Y. Koyama, *Physica C* **282-287**, 1071 (1997).
- [234] Y. Zhu, A. R. Moodenbaugh, Z. X. Cai, J. Taftø, M. Suenaga, and D. O. Welch, *Phys. Rev. Lett.* **73**, 3026 (1994).
- [235] H. Kimura, M. Kofu, Y. Matsumoto, and K. Hirota, *Phys. Rev. Lett.* **91**, 067002 (2003).
- [236] M. Kofu, H. Kimura, and K. Hirota, *Phys. Rev. B* **72**, 064502 (2005).
- [237] H. Kimura, K. Hirota, H. Matsushita, K. Yamada, Y. Endoh, S.-H. Lee, C. F. Majkrzak, R. Erwin, G. Shirane, M. Greven, et al., *Phys. Rev. B* **59**, 6517 (1999).

- [238] S. Wakimoto, R. J. Birgeneau, A. Kagedan, H. Kim, I. Swainson, K. Yamada, and H. Zhang, *Phys. Rev. B* **72**, 064521 (2005).
- [239] Y. Sidis, P. Bourges, B. Hennion, L. P. Regnault, R. Villeneuve, G. Collin, and J. F. Marucco, *Phys. Rev. B* **53**, 6811 (1996).
- [240] K. Kakurai, S. Shamoto, T. Kiyokura, M. Sato, J. M. Tranquada, and G. Shirane, *Phys. Rev. B* **48**, 3485 (1993).
- [241] Y. Sidis, P. Bourges, H. F. Fong, B. Keimer, L. P. Regnault, J. Bossy, A. Ivanov, B. Hennion, P. Gautier-Picard, G. Collin, et al., *Phys. Rev. Lett.* **84**, 5900 (2000).
- [242] B. Nachumi, A. Keren, K. Kojima, M. Larkin, G. M. Luke, J. Merrin, O. Tchernyshöv, Y. J. Uemura, N. Ichikawa, M. Goto, et al., *Phys. Rev. Lett.* **77**, 5421 (1996).
- [243] T. Sasagawa, P. K. Mang, O. P. Vajk, A. Kapitulnik, and M. Greven, *Phys. Rev. B* **66**, 184512 (2002).
- [244] W. Bao, R. J. McQueeney, R. Heffner, J. L. Sarrao, P. Dai, and J. L. Zarestky, *Phys. Rev. Lett.* **84**, 3978 (2000).
- [245] W. Bao, Y. Chen, Y. Qiu, and J. L. Sarrao, *Phys. Rev. Lett.* **91**, 127005 (2003).
- [246] G. M. L. *et al.*, *Phys. Rev. B* **42**, 7981 (1990).
- [247] T. R. Thurston, M. Matsuda, K. Kakurai, K. Yamada, Y. Endoh, R. J. Birgeneau, P. M. Gehring, Y. Hidaka, M. A. Kastner, T. Murakami, et al., *Phys. Rev. Lett.* **65**, 263 (1990).
- [248] I. A. Zobjkalo, A. G. Gukasov, S. Y. Kokovin, S. N. Barilo, and D. I. Zhigunov, *Solid State Commun.* **80**, 921 (1991).
- [249] M. Matsuda, Y. Endoh, K. Yamada, H. Kojima, I. Tanaka, R. J. Birgeneau, M. A. Kastner, and G. Shirane, *Phys. Rev. B* **45**, 12548 (1992).
- [250] P. K. Mang, O. P. Vajk, A. Arvanitaki, J. W. Lynn, and M. Greven, *Phys. Rev. Lett.* **93**, 027002 (2004).
- [251] P. K. Mang, S. Larochelle, and M. Greven, *Nature* **426**, 139 (2003).
- [252] P. K. Mang, S. Larochelle, A. Mehta, O. P. Vajk, A. S. Erickson, L. Lu, W. L. Buyers, A. F. Marshall, K. Prokes, and M. Greven, *Phys. Rev. B* **70**, 094507 (2004).
- [253] K. Yamada, K. Kurahashi, T. Uefuji, M. Fujita, S. Park, S.-H. Lee, and Y. Endoh, *Phys. Rev. Lett.* **90**, 137004 (2003).
- [254] W. Henggeler, G. Cuntze, J. Mesot, M. Klauda, G. Saemann-Ischenko, and A. Furrer, *Europhys. Lett.* **29**, 233 (1995).
- [255] F. Zamborszky, G. Wu, J. Shinagawa, W. Yu, H. Balci, R. L. Greene, W. G. Clark, and S. E. Brown, *Phys. Rev. Lett.* **92**, 047003 (2004).
- [256] O. N. Bakharev, I. M. Abu-Shiekah, H. B. Brom, A. A. Nugroho, I. P. McCulloch, and J. Zaanen, *Phys. Rev. Lett.* **93**, 037002 (2004).
- [257] M. Matsuda, S. Katano, T. Uefuji, M. Fujita, and K. Yamada, *Phys. Rev. B* **66**, 172509 (2002).
- [258] H. J. Kang, P. Dai, J. W. Lynn, M. Matsuura, J. R. Thompson, S.-C. Zhang, D. N. Argyriou, Y. Onose, and Y. Tokura, *Nature* **423**, 522 (2003).

- [259] M. Matsuura, P. Dai, H. J. Kang, J. W. Lynn, D. N. Argyriou, K. Prokes, Y. Onose, and Y. Tokura, *Phys. Rev. B* **68**, 144503 (2003).
- [260] M. Matsuura, P. Dai, H. J. Kang, J. W. Lynn, D. N. Argyriou, Y. Onose, and Y. Tokura, *Phys. Rev. B* **69**, 104510 (2004).
- [261] M. Fujita, M. Matsuda, S. Katano, and K. Yamada, *Phys. Rev. Lett.* **93**, 147003 (2005).
- [262] P. Dai, H. J. Kang, H. A. Mook, M. Matsuura, J. W. Lynn, Y. Kurita, S. Komiya, and Y. Ando, *Phys. Rev. B* **71**, 100502(R) (2005).
- [263] H. J. Kang, P. Dai, H. A. Mook, D. N. Argyriou, V. Sikolenko, J. W. Lynn, Y. Kurita, S. Komiya, and Y. Ando, *Phys. Rev. B* **71**, 214512 (2005).
- [264] Y.-J. Kao, Q. Si, and K. Levin, *Phys. Rev. B* **61**, R11898 (2000).
- [265] M. R. Norman, *Phys. Rev. B* **61**, 14751 (2000).
- [266] J. Brinckmann and P. A. Lee, *Phys. Rev. Lett.* **82**, 2915 (1999).
- [267] A. V. Chubukov, B. Jankó, and O. Tchernyshyov, *Phys. Rev. B* **63**, 180507R (2001).
- [268] I. Eremin and D. Manske, *Phys. Rev. Lett.* **94**, 067006 (2005).
- [269] I. Eremin, D. K. Morr, A. V. Chubukov, K. H. Bennemann, and M. R. Norman, *Phys. Rev. Lett.* **94**, 147001 (2005).
- [270] P. W. Anderson, P. A. Lee, M. Randeria, T. M. Rice, N. Trivedi, and F. C. Zhang, *J. Phys. Condens. Matter* **16**, R755 (2004).
- [271] P. A. Lee, N. Nagaosa, and X.-G. Wen, *Rev. Mod. Phys.* **78** (2006), [cond-mat/0410445](#).
- [272] B. I. Shraiman and E. D. Siggia, *Phys. Rev. Lett.* **62**, 1564 (1989).
- [273] N. Hasselmann, A. H. Castro Neto, and C. Morais Smith, *Phys. Rev. B* **69**, 014424 (2004).
- [274] O. P. Sushkov and V. N. Kotov, *Phys. Rev. B* **70**, 024503 (2004).
- [275] P.-A. Lindgård, *Phys. Rev. Lett.* **95**, 217001 (2005).
- [276] P. Abbamonte, A. Rusydi, S. Smadici, G. D. Gu, G. A. Sawatzky, and D. L. Feng, *Nature Physics* **1**, 155 (2005).
- [277] J. Zaanen, O. Y. Osman, H. V. Kruis, Z. Nussinov, and J. Tworzydło, *Phil. Mag. B* **81**, 1485 (2001).
- [278] S. Sachdev and N. Read, *Int. J. Mod. Phys. B* **5**, 219 (1991).
- [279] K. Machida, *Physica C* **158**, 192 (1989).
- [280] S. A. Kivelson and E. Fradkin (2005), [cond-mat/0507459](#).
- [281] S. A. Kivelson and V. J. Emery, *Synth. Met.* **80**, 151 (1996).
- [282] H. V. Kruis, I. P. McCulloch, Z. Nussinov, and J. Zaanen, *Phys. Rev. B* **70**, 075109 (2004).